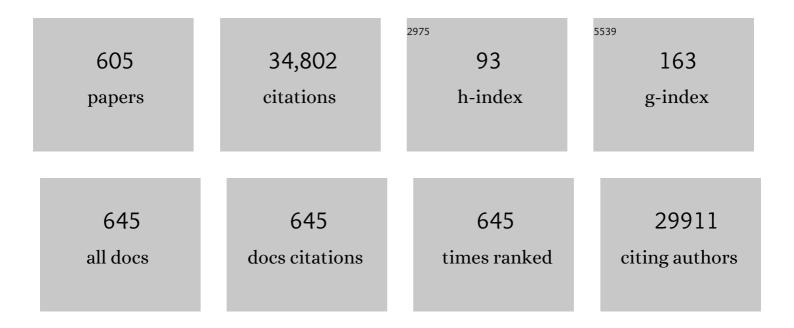
Ru-Shi Liu

List of Publications by Year in descending order

Source: https://exaly.com/author-pdf/3013822/publications.pdf Version: 2024-02-01



RU-SHI LU

#	Article	IF	CITATIONS
1	Single platinum atoms immobilized on an MXene as an efficient catalyst for the hydrogen evolution reaction. Nature Catalysis, 2018, 1, 985-992.	34.4	1,236
2	Plasmonic photocatalysis. Reports on Progress in Physics, 2013, 76, 046401.	20.1	1,140
3	Advances in Phosphors for Light-emitting Diodes. Journal of Physical Chemistry Letters, 2011, 2, 1268-1277.	4.6	1,099
4	Highly efficient non-rare-earth red emitting phosphor for warm white light-emitting diodes. Nature Communications, 2014, 5, 4312.	12.8	1,069
5	Mesoporous Silica Particles Integrated with Allâ€Inorganic CsPbBr ₃ Perovskite Quantumâ€Dot Nanocomposites (MPâ€PQDs) with High Stability and Wide Color Gamut Used for Backlight Display. Angewandte Chemie - International Edition, 2016, 55, 7924-7929.	13.8	730
6	Tuning the Coordination Environment in Single-Atom Catalysts to Achieve Highly Efficient Oxygen Reduction Reactions. Journal of the American Chemical Society, 2019, 141, 20118-20126.	13.7	683
7	Nano-architecture and material designs for water splitting photoelectrodes. Chemical Society Reviews, 2012, 41, 5654.	38.1	483
8	Light Converting Inorganic Phosphors for White Light-Emitting Diodes. Materials, 2010, 3, 2172-2195.	2.9	480
9	Tunable Blue-Green Color Emission and Energy Transfer of Ca ₂ Al ₃ O ₆ F:Ce ³⁺ ,Tb ³⁺ Phosphors for Near-UV White LEDs. Journal of Physical Chemistry C, 2012, 116, 15604-15609.	3.1	445
10	The triggering of apoptosis in macrophages by pristine graphene through the MAPK and TGF-beta signaling pathways. Biomaterials, 2012, 33, 402-411.	11.4	444
11	The Effect of Surface Coating on Energy Migration-Mediated Upconversion. Journal of the American Chemical Society, 2012, 134, 20849-20857.	13.7	405
12	Critical Red Components for Next-Generation White LEDs. Journal of Physical Chemistry Letters, 2016, 7, 495-503.	4.6	401
13	Versatile Phosphate Phosphors ABPO ₄ in White Light-Emitting Diodes: Collocated Characteristic Analysis and Theoretical Calculations. Journal of the American Chemical Society, 2010, 132, 3020-3028.	13.7	324
14	Thermally stable luminescence of KSrPO4:Eu2+ phosphor for white light UV light-emitting diodes. Applied Physics Letters, 2007, 90, 151108.	3.3	313
15	Plasmon Inducing Effects for Enhanced Photoelectrochemical Water Splitting: X-ray Absorption Approach to Electronic Structures. ACS Nano, 2012, 6, 7362-7372.	14.6	307
16	Super Broadband Near-Infrared Phosphors with High Radiant Flux as Future Light Sources for Spectroscopy Applications. ACS Energy Letters, 2018, 3, 2679-2684.	17.4	286
17	Origin of Thermal Degradation of Sr _{2–<i>x</i>} Si ₅ N ₈ :Eu _{<i>x</i>} Phosphors in Air for Light-Emitting Diodes. Journal of the American Chemical Society, 2012, 134, 14108-14117.	13.7	278
18	Ca2Al3O6F:Eu2+: a green-emitting oxyfluoride phosphor for white light-emitting diodes. Journal of Materials Chemistry, 2012, 22, 15183.	6.7	267

#	Article	IF	CITATIONS
19	A Study on the Luminescence and Energy Transfer of Single-Phase and Color-Tunable KCaY(PO ₄) ₂ :Eu ²⁺ ,Mn ²⁺ Phosphor for Application in White-Light LEDs. Inorganic Chemistry, 2012, 51, 9636-9641.	4.0	260
20	Quantum Dot Monolayer Sensitized ZnO Nanowireâ€Array Photoelectrodes: True Efficiency for Water Splitting. Angewandte Chemie - International Edition, 2010, 49, 5966-5969.	13.8	254
21	Photoluminescence Tuning via Cation Substitution in Oxonitridosilicate Phosphors: DFT Calculations, Different Site Occupations, and Luminescence Mechanisms. Chemistry of Materials, 2014, 26, 2991-3001.	6.7	244
22	Perovskite Quantum Dots and Their Application in Lightâ€Emitting Diodes. Small, 2018, 14, 1702433.	10.0	238
23	Harnessing the interplay of Fe–Ni atom pairs embedded in nitrogen-doped carbon for bifunctional oxygen electrocatalysis. Nano Energy, 2020, 71, 104597.	16.0	231
24	Biocompatibility of Fe ₃ O ₄ nanoparticles evaluated by <i>in vitro</i> cytotoxicity assays using normal, glia and breast cancer cells. Nanotechnology, 2010, 21, 075102.	2.6	230
25	High-Performance Lithium-Ion Battery and Symmetric Supercapacitors Based on FeCo ₂ O ₄ Nanoflakes Electrodes. ACS Applied Materials & Interfaces, 2014, 6, 22701-22708.	8.0	230
26	Narrow Red Emission Band Fluoride Phosphor KNaSiF ₆ :Mn ⁴⁺ for Warm White Light-Emitting Diodes. ACS Applied Materials & Interfaces, 2016, 8, 11194-11203.	8.0	228
27	Recent Advancements in Li-Ion Conductors for All-Solid-State Li-Ion Batteries. ACS Energy Letters, 2017, 2, 2734-2751.	17.4	226
28	Nano–bio effects: interaction of nanomaterials with cells. Nanoscale, 2013, 5, 3547.	5.6	223
29	Emission-Tunable CuInS ₂ /ZnS Quantum Dots: Structure, Optical Properties, and Application in White Light-Emitting Diodes with High Color Rendering Index. ACS Applied Materials & Interfaces, 2014, 6, 15379-15387.	8.0	222
30	Hollow Platinum Spheres with Nano-Channels: Synthesis and Enhanced Catalysis for Oxygen Reduction. Journal of Physical Chemistry C, 2008, 112, 7522-7526.	3.1	220
31	Recent advances in quantum dot-based light-emitting devices: Challenges and possible solutions. Materials Today, 2019, 24, 69-93.	14.2	213
32	Cation-Size-Mismatch Tuning of Photoluminescence in Oxynitride Phosphors. Journal of the American Chemical Society, 2012, 134, 8022-8025.	13.7	207
33	Seedless, silver-induced synthesis of star-shaped gold/silver bimetallic nanoparticles as high efficiency photothermal therapy reagent. Journal of Materials Chemistry, 2012, 22, 2244-2253.	6.7	205
34	Super-Hydrophobic Cesium Lead Halide Perovskite Quantum Dot-Polymer Composites with High Stability and Luminescent Efficiency for Wide Color Gamut White Light-Emitting Diodes. Chemistry of Materials, 2019, 31, 1042-1047.	6.7	203
35	Structural Ordering and Charge Variation Induced by Cation Substitution in (Sr,Ca)AlSiN ₃ :Eu Phosphor. Journal of the American Chemical Society, 2015, 137, 8936-8939.	13.7	198
36	Neighboring-Cation Substitution Tuning of Photoluminescence by Remote-Controlled Activator in Phosphor Lattice. Journal of the American Chemical Society, 2013, 135, 12504-12507.	13.7	191

#	Article	IF	CITATIONS
37	Enhanced Photoluminescence Emission and Thermal Stability from Introduced Cation Disorder in Phosphors. Journal of the American Chemical Society, 2017, 139, 11766-11770.	13.7	190
38	Synthesis of Na ₂ SiF ₆ :Mn ⁴⁺ red phosphors for white LED applications by co-precipitation. Journal of Materials Chemistry C, 2014, 2, 10268-10272.	5.5	187
39	Ternary Spinel MCo ₂ O ₄ (M = Mn, Fe, Ni, and Zn) Porous Nanorods as Bifunctional Cathode Materials for Lithium–O ₂ Batteries. ACS Applied Materials & Interfaces, 2015, 7, 12038-12046.	8.0	186
40	Ca1â^'xLixAl1â^'xSi1+xN3:Eu2+ solid solutions as broadband, color-tunable and thermally robust red phosphors for superior color rendition white light-emitting diodes. Light: Science and Applications, 2016, 5, e16155-e16155.	16.6	186
41	A low-temperature co-precipitation approach to synthesize fluoride phosphors K ₂ MF ₆ :Mn ⁴⁺ (M = Ge, Si) for white LED applications. Journal of Materials Chemistry C, 2015, 3, 1655-1660.	5.5	182
42	Effects of Defects on Photocatalytic Activity of Hydrogen-Treated Titanium Oxide Nanobelts. ACS Catalysis, 2017, 7, 1742-1748.	11.2	173
43	High Color Rendering Index of Rb ₂ GeF ₆ :Mn ⁴⁺ for Light-Emitting Diodes. Chemistry of Materials, 2017, 29, 935-939.	6.7	172
44	Highly Stable Red Oxynitride β-SiAlON:Pr ³⁺ Phosphor for Light-Emitting Diodes. Chemistry of Materials, 2011, 23, 3698-3705.	6.7	171
45	Silicon Anode Design for Lithium-Ion Batteries: Progress and Perspectives. Journal of Physical Chemistry C, 2017, 121, 27775-27787.	3.1	169
46	Evolutionary Generation of Phosphor Materials and Their Progress in Future Applications for Light-Emitting Diodes. Chemical Reviews, 2022, 122, 11474-11513.	47.7	167
47	Local Structure and First Cycle Redox Mechanism of Layered Li[sub 1.2]Cr[sub 0.4]Mn[sub 0.4]O[sub 2] Cathode Material. Journal of the Electrochemical Society, 2002, 149, A431.	2.9	165
48	Synthesis, Crystal Structure, and Luminescence Properties of a Novel Green-Yellow Emitting Phosphor LiZn _{1â^'<i>x</i>} PO ₄ :Mn _{<i>x</i>} for Light Emitting Diodes. Chemistry of Materials, 2008, 20, 1215-1217.	6.7	165
49	Ni@NiO Core–Shell Structure-Modified Nitrogen-Doped InTaO ₄ for Solar-Driven Highly Efficient CO ₂ Reduction to Methanol. Journal of Physical Chemistry C, 2011, 115, 10180-10186.	3.1	165
50	Controlling The Activator Site To Tune Europium Valence in Oxyfluoride Phosphors. Chemistry of Materials, 2012, 24, 2220-2227.	6.7	164
51	Robust and Stable Narrow-Band Green Emitter: An Option for Advanced Wide-Color-Gamut Backlight Display. Chemistry of Materials, 2016, 28, 8493-8497.	6.7	164
52	Perovskite Quantum Dots for Application in High Color Gamut Backlighting Display of Light-Emitting Diodes. ACS Energy Letters, 2020, 5, 3374-3396.	17.4	162
53	Nitrate reduction to ammonium: from CuO defect engineering to waste NO _x -to-NH ₃ economic feasibility. Energy and Environmental Science, 2021, 14, 3588-3598.	30.8	161
54	Waterproof Alkyl Phosphate Coated Fluoride Phosphors for Optoelectronic Materials. Angewandte Chemie - International Edition, 2015, 54, 10862-10866.	13.8	160

#	Article	IF	CITATIONS
55	Architecture of Metallic Nanostructures: Synthesis Strategy and Specific Applications. Journal of Physical Chemistry C, 2011, 115, 3513-3527.	3.1	156
56	Unraveling the effect of salt chemistry on long-durability high-phosphorus-concentration anode for potassium ion batteries. Nano Energy, 2018, 53, 967-974.	16.0	151
57	Penetrating Biological Tissue Using Light-Emitting Diodes with a Highly Efficient Near-Infrared ScBO ₃ :Cr ³⁺ Phosphor. Chemistry of Materials, 2020, 32, 2166-2171.	6.7	142
58	Plasmonic hot electrons for sensing, photodetection, and solar energy applications: A perspective. Journal of Chemical Physics, 2020, 152, 220901.	3.0	141
59	Combinatorial Approach to the Development of a Single Mass YVO ₄ :Bi ³⁺ ,Eu ³⁺ Phosphor with Red and Green Dual Colors for High Color Rendering White Light-Emitting Diodes. ACS Combinatorial Science, 2010, 12, 587-594.	3.3	140
60	Green Light-Excitable Ce-Doped Nitridomagnesoaluminate Sr[Mg ₂ Al ₂ N ₄] Phosphor for White Light-Emitting Diodes. Chemistry of Materials, 2016, 28, 6822-6825.	6.7	138
61	Narrow-band red-emitting Mn ⁴⁺ -doped hexafluoride phosphors: synthesis, optoelectronic properties, and applications in white light-emitting diodes. Journal of Materials Chemistry C, 2016, 4, 10759-10775.	5.5	138
62	Heterostructure of Si and CoSe ₂ : A Promising Photocathode Based on a Nonâ€noble Metal Catalyst for Photoelectrochemical Hydrogen Evolution. Angewandte Chemie - International Edition, 2015, 54, 6211-6216.	13.8	134
63	Photoluminescent Evolution Induced by Structural Transformation Through Thermal Treating in the Red Narrow-Band Phosphor K ₂ GeF ₆ :Mn ⁴⁺ . ACS Applied Materials & Interfaces, 2015, 7, 10656-10659.	8.0	133
64	Highâ€Performance CsPb _{1â^'<i>x</i>} Sn _{<i>x</i>} Br ₃ Perovskite Quantum Dots for Lightâ€Emitting Diodes. Angewandte Chemie - International Edition, 2017, 56, 13650-13654.	13.8	133
65	Impact of Lanthanide Nanomaterials on Photonic Devices and Smart Applications. Small, 2018, 14, e1801882.	10.0	128
66	Synthesis and Luminescent Properties of a New Yellowish-Orange Afterglow Phosphor Y2O2S:Ti,Mg. Chemistry of Materials, 2003, 15, 3966-3968.	6.7	127
67	An oleic acid-capped CdSe quantum-dot sensitized solar cell. Applied Physics Letters, 2009, 94, .	3.3	126
68	Biosensing, Cytotoxicity, and Cellular Uptake Studies of Surface-Modified Gold Nanorods. Journal of Physical Chemistry C, 2009, 113, 7574-7578.	3.1	126
69	Chromium Ion Pair Luminescence: A Strategy in Broadband Near-Infrared Light-Emitting Diode Design. Journal of the American Chemical Society, 2021, 143, 19058-19066.	13.7	125
70	Cadmiumâ€Free InP/ZnSeS/ZnS Heterostructureâ€Based Quantum Dot Lightâ€Emitting Diodes with a ZnMgO Electron Transport Layer and a Brightness of Over 10 000 cd m ^{â^'2} . Small, 2017, 13, 1603962.	10.0	124
71	An efficient multi-doping strategy to enhance Li-ion conductivity in the garnet-type solid electrolyte Li ₇ La ₃ Zr ₂ O ₁₂ . Journal of Materials Chemistry A, 2019, 7, 8589-8601.	10.3	124
72	Strategies for Designing Antithermalâ€Quenching Red Phosphors. Advanced Science, 2020, 7, 1903060.	11.2	121

#	Article	IF	CITATIONS
73	Facile Atmospheric Pressure Synthesis of High Thermal Stability and Narrow-Band Red-Emitting SrLiAl ₃ N ₄ :Eu ²⁺ Phosphor for High Color Rendering Index White Light-Emitting Diodes. ACS Applied Materials & Interfaces, 2016, 8, 19612-19617.	8.0	120
74	Control of Narrow-Band Emission in Phosphor Materials for Application in Light-Emitting Diodes. ACS Energy Letters, 2018, 3, 2573-2586.	17.4	118
75	Eu^2+-activated silicon-oxynitride Ca_3Si_2O_4N_2: a green-emitting phosphor for white LEDs. Optics Express, 2011, 19, A331.	3.4	115
76	The Study of Nanocrystalline Cerium Oxide by X-Ray Absorption Spectroscopy. Journal of Solid State Chemistry, 2000, 149, 408-413.	2.9	112
77	Ultra-high-efficiency near-infrared Ga ₂ O ₃ :Cr ³⁺ phosphor and controlling of phytochrome. Journal of Materials Chemistry C, 2020, 8, 11013-11017.	5.5	111
78	Hidden Structural Evolution and Bond Valence Control in Near-Infrared Phosphors for Light-Emitting Diodes. ACS Energy Letters, 2021, 6, 109-114.	17.4	110
79	KBaPO4:Ln (Ln=Eu, Tb, Sm) phosphors for UV excitable white light-emitting diodes. Journal of Luminescence, 2009, 129, 1682-1684.	3.1	107
80	Diffusional mechanism of deintercalation in LiFe1â^'yMnyPO4 cathode material. Solid State Ionics, 2006, 177, 2617-2624.	2.7	106
81	Highly stable three-band white light from an InGaN-based blue light-emitting diode chip precoated with (oxy)nitride green/red phosphors. Applied Physics Letters, 2007, 90, 123503.	3.3	105
82	[INVITED] Near-infrared phosphors and their full potential: A review on practical applications and future perspectives. Journal of Luminescence, 2020, 219, 116944.	3.1	105
83	Full-Color and Thermally Stable KSrPO[sub 4]:Ln (Ln=Eu,â€,Tb,â€,Sm) Phosphors for White-Light-Emitting Diodes. Journal of the Electrochemical Society, 2008, 155, J248.	2.9	103
84	Near-ultraviolet excitable orange-yellow Sr3(Al2O5)Cl2:Eu2+ phosphor for potential application in light-emitting diodes. Applied Physics Letters, 2008, 93, .	3.3	103
85	O- <i>K</i> and Co- <i>L</i> XANES Study on Oxygen Intercalation in Perovskite SrCoO _{3-Î} . Chemistry of Materials, 2010, 22, 70-76.	6.7	102
86	(Ba,Sr)Y2Si2Al2O2N5 : Eu2+: a novel near-ultraviolet converting green phosphor for white light-emitting diodes. Journal of Materials Chemistry, 2011, 21, 3740.	6.7	100
87	Mesoporous ZnCo2O4 nanoflakes with bifunctional electrocatalytic activities toward efficiencies of rechargeable lithium–oxygen batteries in aprotic media. Nanoscale, 2013, 5, 12115.	5.6	100
88	Synthesis and Characterization of LiFePO[sub 4] and LiTi[sub 0.01]Fe[sub 0.99]PO[sub 4] Cathode Materials. Journal of the Electrochemical Society, 2006, 153, A25.	2.9	99
89	Characterization of core–shell type and alloy Ag/Au bimetallic clusters by using extended X-ray absorption fine structure spectroscopy. Chemical Physics Letters, 2006, 421, 118-123.	2.6	99
90	Preparation of a novel red Rb ₂ SiF ₆ :Mn ⁴⁺ phosphor with high thermal stability through a simple one-step approach. Journal of Materials Chemistry C, 2015, 3, 7277-7280.	5.5	98

#	Article	IF	CITATIONS
91	Determination of Ru valence from x-ray absorption near-edge structure inRuSr2GdCu2O8-type superconductors. Physical Review B, 2001, 63, .	3.2	97
92	The Origin of Capacity Fade in the Li ₂ MnO ₃ ·Li <i>M</i> O ₂ (<i>M</i>) Tj Transmission X-ray Microscopy Study. Journal of the American Chemical Society, 2016, 138, 8824-8833.	ETQq0 0 (13.7	0 rgBT /Overlo 96
93	Enhanced luminescence of SrSi2O2N2:Eu2+ phosphors by codoping with Ce3+, Mn2+, and Dy3+ ions. Applied Physics Letters, 2007, 91, 061119.	3.3	95
94	Broadband Cr ³⁺ , Sn ⁴⁺ â€Doped Oxide Nanophosphors for Infrared Mini Lightâ€Emitting Diodes. Angewandte Chemie - International Edition, 2019, 58, 2069-2072.	13.8	95
95	Minimizing the Heat Effect of Photodynamic Therapy Based on Inorganic Nanocomposites Mediated by 808 nm Nearâ€Infrared Light. Small, 2017, 13, 1700038.	10.0	94
96	Control of Luminescence by Tuning of Crystal Symmetry and Local Structure in Mn ⁴⁺ â€Activated Narrow Band Fluoride Phosphors. Angewandte Chemie - International Edition, 2018, 57, 1797-1801.	13.8	93
97	Nitrogen-doped graphene nanosheet-supported non-precious iron nitride nanoparticles as an efficient electrocatalyst for oxygen reduction. RSC Advances, 2011, 1, 1349.	3.6	91
98	Chemical Pressure Control for Photoluminescence of MSiAl ₂ O ₃ N ₂ :Ce ³⁺ /Eu ²⁺ (M = Sr, Ba) Oxynitride Phosphors. Chemistry of Materials, 2014, 26, 2075-2085.	6.7	91
99	Photocatalytic CdSe QDs-decorated ZnO nanotubes: an effective photoelectrode for splitting water. Chemical Communications, 2011, 47, 3493.	4.1	90
100	Superconductivity up to 90 K in a New Family of the (Pb,Hg)Sr2(Ca,Y)Cu2O7 System. Journal of Solid State Chemistry, 1993, 103, 280-286.	2.9	89
101	Eu substitution and particle size control of Y2O2S for the excitation by UV light emitting diodes. Solid State Communications, 2005, 136, 205-209.	1.9	86
102	A New Approach to Solar Hydrogen Production: a ZnO–ZnS Solid Solution Nanowire Array Photoanode. Advanced Energy Materials, 2011, 1, 742-747.	19.5	86
103	Plasmon-Enhanced Photodynamic Cancer Therapy by Upconversion Nanoparticles Conjugated with Au Nanorods. ACS Applied Materials & Interfaces, 2016, 8, 32108-32119.	8.0	86
104	Superconductivity and the metal-semiconductor transition in the septenary oxide system, (TI0.5Pb0.5)(Ca1â^'yYy)Sr2Cu2O7â^δ. Journal of Solid State Chemistry, 1990, 86, 334-339.	2.9	85
105	Study of electrochemical properties of coating ZrO2 on LiCoO2. Journal of Alloys and Compounds, 2010, 496, 512-516.	5.5	85
106	Enhance Color Rendering Index via Full Spectrum Employing the Important Key of Cyan Phosphor. ACS Applied Materials & Interfaces, 2016, 8, 30677-30682.	8.0	85
107	Improving Optical Properties of White LED Fabricated by a Blue LED Chip with Yellow/Red Phosphors. Journal of the Electrochemical Society, 2010, 157, H900.	2.9	84
108	Chromium(III)-Doped Fluoride Phosphors with Broadband Infrared Emission for Light-Emitting Diodes. Inorganic Chemistry, 2020, 59, 376-385.	4.0	84

#	Article	IF	CITATIONS
109	Synthesis of Y[sub 2]O[sub 3]:Eu, Bi Red Phosphors by Homogeneous Coprecipitation and Their Photoluminescence Behaviors. Journal of the Electrochemical Society, 2005, 152, J93.	2.9	83
110	ZnB_2O_4:Bi^3+,Eu^3+:a highly efficient, red-emitting phosphor. Optics Express, 2010, 18, 2946.	3.4	82
111	Flower-like ZnCo2O4 nanowires: toward a high-performance anode material for Li-ion batteries. RSC Advances, 2013, 3, 20143.	3.6	82
112	Mesoporous Silica Particles Integrated with Allâ€Inorganic CsPbBr ₃ Perovskite Quantumâ€Dot Nanocomposites (MPâ€PQDs) with High Stability and Wide Color Gamut Used for Backlight Display. Angewandte Chemie, 2016, 128, 8056-8061.	2.0	81
113	A study on LiFePO4 and its doped derivatives as cathode materials for lithium-ion batteries. Journal of Power Sources, 2006, 159, 282-286.	7.8	77
114	Evaluations of the Chemical Stability and Cytotoxicity of CulnS ₂ and CulnS ₂ /ZnS Core/Shell Quantum Dots. Journal of Physical Chemistry C, 2015, 119, 2852-2860.	3.1	77
115	Plasmonic ZnO/Ag Embedded Structures as Collecting Layers for Photogenerating Electrons in Solar Hydrogen Generation Photoelectrodes. Small, 2013, 9, 2926-2936.	10.0	76
116	Synthesis of Ag nanospheres particles in ethylene glycol by electrochemical-assisted polyol process. Chemical Physics Letters, 2006, 420, 304-308.	2.6	75
117	Single-phased white-light-emitting Ca ₄ (PO ₄) ₂ O:Ce ³⁺ ,Eu ²⁺ phosphors based on energy transfer. Dalton Transactions, 2015, 44, 11399-11407.	3.3	75
118	Structure, Luminescence, and Application of a Robust Carbidonitride Blue Phosphor (Al _{1–<i>x</i>} Si _{<i>x</i>} C _{<i>x</i>} N _{1–<i>x</i>} :Eu ^{2+ for Near UV-LED Driven Solid State Lighting. Chemistry of Materials, 2015, 27, 8457-8466.}	⊦ 6¦s up>)	75
119	Single 808 nm Laser Treatment Comprising Photothermal and Photodynamic Therapies by Using Gold Nanorods Hybrid Upconversion Particles. Journal of Physical Chemistry C, 2018, 122, 2402-2412.	3.1	74
120	Integrated Surface Modification to Enhance the Luminescence Properties of K ₂ TiF ₆ :Mn ⁴⁺ Phosphor and Its Application in White-Light-Emitting Diodes. ACS Applied Materials & Interfaces, 2018, 10, 29233-29237.	8.0	74
121	Recent Developments in Leadâ€Free Double Perovskites: Structure, Doping, and Applications. Chemistry - an Asian Journal, 2020, 15, 242-252.	3.3	74
122	Combinatorial chemistry approach to searching phosphors for white light-emitting diodes in (Gd-Y-Bi-Eu)VO4 quaternary system. Journal of Materials Chemistry, 2011, 21, 3677.	6.7	73
123	Single-phased white-light-emitting KCaGd(PO4)2:Eu2+,Tb3+,Mn2+ phosphors for LED applications. RSC Advances, 2013, 3, 9023.	3.6	73
124	Graphitic carbon nitride-based nanocomposites and their biological applications: a review. Nanoscale, 2019, 11, 14993-15003.	5.6	72
125	Investigation of the Luminescent Properties of Tb[sup 3+]-Substituted YAG:Ce, Gd Phosphors. Journal of the Electrochemical Society, 2005, 152, J41.	2.9	71
126	Synthesis and Characterization of Multi-Pod-Shaped Gold/Silver Nanostructures. Journal of Physical Chemistry C, 2007, 111, 5909-5914.	3.1	71

#	Article	IF	CITATIONS
127	Voltammetric Enhancement of Li-Ion Conduction in Al-Doped Li _{7–<i>x</i>} La ₃ Zr ₂ O ₁₂ Solid Electrolyte. Journal of Physical Chemistry C, 2017, 121, 15565-15573.	3.1	71
128	Versatile phosphors BaY_2Si_3O_10:RE (RE = Ce^3+, Tb^3+, Eu^3+) for light-emitting diodes. Optics Express, 2009, 17, 18103.	3.4	70
129	Structure, composition, morphology, photoluminescence and cathodoluminescence properties of ZnGeN2 and ZnGeN2:Mn2+ for field emission displays. Acta Materialia, 2010, 58, 6728-6735.	7.9	70
130	Near-Infrared Light-Mediated Photodynamic Therapy Nanoplatform by the Electrostatic Assembly of Upconversion Nanoparticles with Graphitic Carbon Nitride Quantum Dots. Inorganic Chemistry, 2016, 55, 10267-10277.	4.0	69
131	Microfluidic Synthesis of Semiconducting Colloidal Quantum Dots and Their Applications. ACS Applied Nano Materials, 2019, 2, 1773-1790.	5.0	69
132	Transforming active sites in nickel–nitrogen–carbon catalysts for efficient electrochemical CO2 reduction to CO. Nano Energy, 2020, 78, 105213.	16.0	69
133	An integrated cobalt disulfide (CoS ₂) co-catalyst passivation layer on silicon microwires for photoelectrochemical hydrogen evolution. Journal of Materials Chemistry A, 2015, 3, 23466-23476.	10.3	68
134	Designing Undercoordinated Ni–N _{<i>x</i>} and Fe–N _{<i>x</i>} on Holey Graphene for Electrochemical CO ₂ Conversion to Syngas. ACS Nano, 2021, 15, 12006-12018.	14.6	68
135	Ni ²⁺ -Doped Garnet Solid-Solution Phosphor-Converted Broadband Shortwave Infrared Light-Emitting Diodes toward Spectroscopy Application. ACS Applied Materials & Interfaces, 2022, 14, 4265-4275.	8.0	68
136	Controlling the Length and Shape of Gold Nanorods. Journal of Physical Chemistry B, 2005, 109, 19553-19555.	2.6	67
137	Multi-Bandgap-Sensitized ZnO Nanorod Photoelectrode Arrays for Water Splitting: An X-ray Absorption Spectroscopy Approach for the Electronic Evolution under Solar Illumination. Journal of Physical Chemistry C, 2011, 115, 21971-21980.	3.1	67
138	Fast Fabrication of a Ag Nanostructure Substrate Using the Femtosecond Laser for Broad-Band and Tunable Plasmonic Enhancement. ACS Nano, 2012, 6, 5190-5197.	14.6	67
139	Significant Improved Luminescence Intensity of Eu[sup 2+]-Doped Ca[sub 3]SiO[sub 4]Cl[sub 2] Green Phosphor for White LEDs Synthesized Through Two-Stage Method. Journal of the Electrochemical Society, 2009, 156, G29.	2.9	66
140	Ameliorating Interfacial Ionic Transportation in All-Solid-State Li-Ion Batteries with Interlayer Modifications. ACS Energy Letters, 2018, 3, 2775-2795.	17.4	66
141	Combinatorial Study of the Optimization of Y2O3:Bi,Eu Red Phosphors. ACS Combinatorial Science, 2007, 9, 343-346.	3.3	65
142	Particle Size Effect on the Packaging Performance of YAG:Ce Phosphors in White LEDs. International Journal of Applied Ceramic Technology, 2009, 6, 465-469.	2.1	65
143	Effects of additional Ce3+ doping on the luminescence of Li2SrSiO4:Eu2+ yellow phosphor. Applied Physics Letters, 2010, 96, .	3.3	65
144	Plasmon-induced hyperthermia: hybrid upconversion NaYF ₄ :Yb/Er and gold nanomaterials for oral cancer photothermal therapy. Journal of Materials Chemistry B, 2015, 3, 8293-8302.	5.8	65

#	Article	IF	CITATIONS
145	Tunable Nonthermal Distribution of Hot Electrons in a Semiconductor Injected from a Plasmonic Gold Nanostructure. ACS Nano, 2018, 12, 7117-7126.	14.6	65
146	Interfacial chemistry in anode-free batteries: challenges and strategies. Journal of Materials Chemistry A, 2021, 9, 7396-7406.	10.3	65
147	Ultra-Broadband Phosphors Converted Near-Infrared Light Emitting Diode with Efficient Radiant Power for Spectroscopy Applications. ACS Photonics, 2019, 6, 3215-3224.	6.6	64
148	Plasmonic optical properties of a single gold nano-rod. Optics Express, 2007, 15, 7132.	3.4	63
149	A Versatile Route to the Controlled Synthesis of Gold Nanostructures. Crystal Growth and Design, 2009, 9, 2079-2087.	3.0	63
150	Improvement of the Water Resistance of a Narrowâ€Band Redâ€Emitting SrLiAl ₃ N ₄ :Eu ²⁺ Phosphor Synthesized under High Isostatic Pressure through Coating with an Organosilica Layer. Angewandte Chemie - International Edition, 2016, 55, 9652-9656.	13.8	63
151	Critical Review—Narrow-Band Emission of Nitride Phosphors for Light-Emitting Diodes: Perspectives and Opportunities. ECS Journal of Solid State Science and Technology, 2018, 7, R3111-R3133.	1.8	62
152	Interface Between Solid-State Electrolytes and Li-Metal Anodes: Issues, Materials, and Processing Routes. ACS Applied Materials & Interfaces, 2020, 12, 47181-47196.	8.0	62
153	Plasmon-enhanced near-infrared-active materials in photoelectrochemical water splitting. Chemical Communications, 2013, 49, 7917.	4.1	61
154	Efficient energy storage capabilities promoted by hierarchical MnCo2O4 nanowire-based architectures. RSC Advances, 2014, 4, 17230.	3.6	60
155	Optimizing the size and surface properties of polyethylene glycol (PEG)–gold nanoparticles by intense x-ray irradiation. Journal Physics D: Applied Physics, 2008, 41, 195301.	2.8	58
156	Silicon microwire arrays decorated with amorphous heterometal-doped molybdenum sulfide for water photoelectrolysis. Nano Energy, 2017, 32, 422-432.	16.0	58
157	Blue Emission by Interstitial Site Occupation of Ce ³⁺ in AlN. Chemistry of Materials, 2012, 24, 3486-3492.	6.7	57
158	UV/VUV switch-driven color-reversal effect for Tb-activated phosphors. Light: Science and Applications, 2016, 5, e16066-e16066.	16.6	57
159	Controlling of Structural Ordering and Rigidity of β-SiAlON:Eu through Chemical Cosubstitution to Approach Narrow-Band-Emission for Light-Emitting Diodes Application. Chemistry of Materials, 2017, 29, 6781-6792.	6.7	57
160	Structural Evolution and Effect of the Neighboring Cation on the Photoluminescence of Sr(LiAl ₃) _{1â^'<i>x</i>} (SiMg ₃) _{<i>x</i>} N ₄ :Eu <sup Phosphors. Angewandte Chemie - International Edition, 2019, 58, 7767-7772.</sup)> 23.6 /sup	> 57
161	Cuboid-Size-Controlled Color-Tunable Eu-Doped Alkali–Lithosilicate Phosphors. Chemistry of Materials, 2020, 32, 1748-1759.	6.7	56
162	Investigation of Fe valence in LiFePO4 by Mössbauer and XANES spectroscopic techniques. Solid State Communications, 2004, 132, 455-458.	1.9	55

#	Article	IF	CITATIONS
163	Isovalent and aliovalent substitution effects on redox chemistry of Sr2MgMoO6â^î^ SOFC-anode material. Solid State Ionics, 2010, 181, 754-759.	2.7	54
164	The CoTe ₂ nanostructure: an efficient and robust catalyst for hydrogen evolution. Chemical Communications, 2015, 51, 17012-17015.	4.1	54
165	Targeting polymeric fluorescent nanodiamond-gold/silver multi-functional nanoparticles as a light-transforming hyperthermia reagent for cancer cells. Nanoscale, 2013, 5, 3931.	5.6	53
166	Nanobubble-embedded inorganic 808Ânm excited upconversion nanocomposites for tumor multiple imaging and treatment. Chemical Science, 2018, 9, 3141-3151.	7.4	53
167	Superconductivity with Tc(zero) above 105 K in Tl-containing septenary oxides with Y1Ba2Cu3Oy-like structure. Physica C: Superconductivity and Its Applications, 1990, 165, 347-353.	1.2	51
168	Magnetic structure and spin reorientation of the Mn ions in NdMnO3. Journal of Applied Physics, 2000, 87, 5822-5824.	2.5	51
169	A new green phosphor of SrAl2O4:Eu2+,Ce3+,Li+ for alternating current driven light-emitting diodes. Materials Research Bulletin, 2012, 47, 4071-4075.	5.2	51
170	Disorder–Order Conversionâ€Induced Enhancement of Thermal Stability of Pyroxene Nearâ€Infrared Phosphors for Lightâ€Emitting Diodes. Angewandte Chemie - International Edition, 2022, 61, .	13.8	51
171	A new 92 K high-Tc superconductor. Physica C: Superconductivity and Its Applications, 1993, 205, 206-211.	1.2	50
172	Generating Isotropic Superparamagnetic Interconnectivity for the Two-Dimensional Organization of Nanostructured Building Blocks. Angewandte Chemie - International Edition, 2006, 45, 2713-2717.	13.8	50
173	Temperature Dependent Emission of Strontium-Barium Orthosilicate (Sr _{2â~x} Ba _x)SiO ₄ :Eu ₂₊ Phosphors for High-Power White Light-Emitting Diodes. Journal of the Electrochemical Society, 2011, 158, P118-P121.	2.9	50
174	All-Solid-State Li-Ion Battery Using Li _{1.5} Al _{0.5} Ge _{1.5} (PO ₄) ₃ As Electrolyte Without Polymer Interfacial Adhesion. Journal of Physical Chemistry C, 2018, 122, 14383-14389.	3.1	50
175	Aluminate Red Phosphor in Light-Emitting Diodes: Theoretical Calculations, Charge Varieties, and High-Pressure Luminescence Analysis. ACS Applied Materials & Interfaces, 2017, 9, 23995-24004.	8.0	49
176	Continuous Synthesis of Highly Stable Cs ₄ PbBr ₆ Perovskite Microcrystals by a Microfluidic System and Their Application in White-Light-Emitting Diodes. Inorganic Chemistry, 2018, 57, 13071-13074.	4.0	49
177	CoSe ₂ Embedded in C ₃ N ₄ : An Efficient Photocathode for Photoelectrochemical Water Splitting. ACS Applied Materials & Interfaces, 2016, 8, 26690-26696.	8.0	48
178	Investigation of the Growth Mechanism of Iron Oxide Nanoparticles via a Seed-Mediated Method and Its Cytotoxicity Studies. Journal of Physical Chemistry C, 2008, 112, 15684-15690.	3.1	47
179	Near-Infrared Quantum Cutting Platform in Thermally Stable Phosphate Phosphors for Solar Cells. Inorganic Chemistry, 2013, 52, 7352-7357.	4.0	47
180	Theranostic nanobubble encapsulating a plasmon-enhanced upconversion hybrid nanosystem for cancer therapy. Theranostics, 2020, 10, 782-796.	10.0	46

Ru-Sнı Lıu

#	Article	IF	CITATIONS
181	Singleâ€Crystal Red Phosphors and Their Core–Shell Structure for Improved Waterâ€Resistance for Laser Diodes Applications. Angewandte Chemie - International Edition, 2021, 60, 3940-3945.	13.8	46
182	Equilibrium phase relations in the Bi–Ca–Sr–Cu–O system at 850 and 900°C. Journal of Materials Research, 1990, 5, 1403-1408.	2.6	45
183	Characterisation of olivine-type LiMnxFe1â^'xPO4 cathode materials. Journal of Alloys and Compounds, 2006, 425, 362-366.	5.5	45
184	Effect of Co doping in LiMn2O4. Journal of Power Sources, 2001, 102, 21-28.	7.8	44
185	A novel CO-tolerant PtRu core–shell structured electrocatalyst with Ru rich in core and Pt rich in shell for hydrogen oxidation reaction and its implication in proton exchange membrane fuel cell. Journal of Power Sources, 2011, 196, 9117-9123.	7.8	44
186	Nanosegregation and Neighbor ation Control of Photoluminescence in Carbidonitridosilicate Phosphors. Angewandte Chemie - International Edition, 2013, 52, 8102-8106.	13.8	44
187	Ru valence inRuSr2Gd2â^'xCexCu2O10+Î′as measured by x-ray-absorption near-edge spectroscopy. Physical Review B, 2002, 65, .	3.2	43
188	Controlling Length of Gold Nanowires with Large-Scale:  X-ray Absorption Spectroscopy Approaches to the Growth Process. Journal of Physical Chemistry C, 2007, 111, 18550-18557.	3.1	43
189	An alternative cobalt oxide-supported platinum catalyst for efficient hydrolysis of sodium borohydride. Journal of Materials Chemistry, 2011, 21, 11754.	6.7	43
190	Ultrafast Self-Crystallization of High-External-Quantum-Efficient Fluoride Phosphors for Warm White Light-Emitting Diodes. ACS Applied Materials & Interfaces, 2018, 10, 17508-17511.	8.0	43
191	Appropriate green phosphor of SrSi_2O_2N_2:Eu^2+,Mn^2+ for AC LEDs. Optics Express, 2012, 20, 18031.	3.4	42
192	MMP2-sensing up-conversion nanoparticle for fluorescence biosensing in head and neck cancer cells. Biosensors and Bioelectronics, 2016, 80, 131-139.	10.1	42
193	Multi-Site Cation Control of Ultra-Broadband Near-Infrared Phosphors for Application in Light-Emitting Diodes. Inorganic Chemistry, 2020, 59, 15101-15110.	4.0	42
194	Thermally Stable and Deep Red Luminescence of Sr _{1–<i>x</i>} Ba _{<i>x</i>} [Mg ₂ Al ₂ N ₄]:Eu ^{ (<i>x</i> = 0–1) Phosphors for Solid State and Agricultural Lighting Applications. ACS Applied Materials & Interfaces, 2020, 12, 23165-23171.}	2+	42
195	An Advanced <i>In Situ</i> Magnetic Resonance Imaging and Ultrasonic Theranostics Nanocomposite Platform: Crossing the Blood†Brain Barrier and Improving the Suppression of Glioblastoma Using Iron-Platinum Nanoparticles in Nanobubbles. ACS Applied Materials & amp; Interfaces, 2021, 13, 26759-26769.	8.0	42
196	Nitrogen-inserted nickel nanosheets with controlled orbital hybridization and strain fields for boosted hydrogen oxidation in alkaline electrolytes. Energy and Environmental Science, 2022, 15, 1234-1242.	30.8	42
197	Size effects in the NMR of SnO2 powders. Materials Research Bulletin, 1999, 34, 1513-1520.	5.2	41
198	Development of wavelet de-noising technique for PET images. Computerized Medical Imaging and Graphics, 2005, 29, 297-304.	5.8	41

#	Article	IF	CITATIONS
199	Array of CdSe QD-Sensitized ZnO Nanorods Serves as Photoanode for Water Splitting. Journal of the Electrochemical Society, 2010, 157, B1430.	2.9	41
200	Crystal and local structure refinement in Ca ₂ Al ₃ O ₆ F explored by X-ray diffraction and Raman spectroscopy. Physical Chemistry Chemical Physics, 2014, 16, 5952-5957.	2.8	41
201	Highâ€Performance CsPb _{1â^'<i>x</i>} Sn _{<i>x</i>} Br ₃ Perovskite Quantum Dots for Lightâ€Emitting Diodes. Angewandte Chemie, 2017, 129, 13838-13842.	2.0	41
202	ZnO nanorod optical disk photocatalytic reactor for photodegradation of methyl orange. Optics Express, 2013, 21, 7240.	3.4	40
203	Phosphorous-doped molybdenum disulfide anchored on silicon as an efficient catalyst for photoelectrochemical hydrogen generation. Applied Catalysis B: Environmental, 2020, 263, 118259.	20.2	40
204	Iron valence in double-perovskite (Ba,Sr,Ca)2FeMoO6: isovalent substitution effect. Journal of Solid State Chemistry, 2004, 177, 2655-2662.	2.9	39
205	Fabrication and magnetic properties of nickel nanowires. Journal of Magnetism and Magnetic Materials, 2004, 282, 28-31.	2.3	39
206	Preparation and properties of bio-compatible magnetic Fe3O4 nanoparticles. Journal of Magnetism and Magnetic Materials, 2006, 304, e415-e417.	2.3	39
207	Controlling Optical Properties of Aluminum Oxide Using Electrochemical Deposition. Journal of the Electrochemical Society, 2007, 154, K11.	2.9	39
208	Synergistic-Effect-Controlled CoTe ₂ /Carbon Nanotube Hybrid Material for Efficient Water Oxidation. Journal of Physical Chemistry C, 2016, 120, 28093-28099.	3.1	39
209	X-ray Absorption Studies in Spinel-Type LiMn2O4. Journal of Solid State Chemistry, 1997, 128, 326-329.	2.9	38
210	Fabrication of Nanorattles with Passive Shell. Journal of Physical Chemistry B, 2006, 110, 19162-19167.	2.6	38
211	Chemical substitution effects of Tb3+ in YAG:Ce phosphors and enhancement of their emission intensity using flux combination. Journal of Luminescence, 2007, 122-123, 580-582.	3.1	38
212	Ferromagnetic CoPt ₃ Nanowires: Structural Evolution from fcc to Ordered L1 ₂ . Journal of the American Chemical Society, 2009, 131, 15794-15801.	13.7	38
213	CdSe/ZnS QD@CNT nanocomposite photocathode for improvement on charge overpotential in photoelectrochemical Li-O2 batteries. Chemical Engineering Journal, 2018, 349, 235-240.	12.7	38
214	Surface-Protected High-Efficiency Nanophosphors via Space-Limited Ship-in-a-Bottle Synthesis for Broadband Near-Infrared Mini-Light-Emitting Diodes. ACS Energy Letters, 2021, 6, 659-664.	17.4	38
215	Improvement efficiency of a dye-sensitized solar cell using Eu3+ modified TiO2 nanoparticles as a secondary layer electrode. Journal of Materials Chemistry, 2010, 20, 6505.	6.7	37
216	Improvement of emission efficiency and color rendering of high-power LED by controlling size of phosphor particles and utilization of different phosphors. Microelectronics Reliability, 2012, 52, 900-904.	1.7	37

#	Article	IF	CITATIONS
217	Advanced sensing, imaging, and therapy nanoplatforms based on Nd ³⁺ -doped nanoparticle composites exhibiting upconversion induced by 808 nm near-infrared light. Nanoscale, 2017, 9, 18153-18168.	5.6	37
218	Chemical Control of SrLi(Al _{1–<i>x</i>} Ga <i>_x</i>) ₃ N ₄ :Eu ²⁺ Red Phosphors at Extreme Conditions for Application in Light-Emitting Diodes. Chemistry of Materials, 2019, 31, 4614-4618.	6.7	37
219	Spinel Zinc Cobalt Oxide (ZnCo ₂ O ₄) Porous Nanorods as a Cathode Material for Highly Durable Li–CO ₂ Batteries. ACS Applied Materials & Interfaces, 2020, 12, 17353-17363.	8.0	37
220	Pressure dependence of the superconducting critical temperature ofTl2Ba2Ca2Cu3O10+yandTl2Ba2Ca3Cu4O12+yup to 21 GPa. Physical Review B, 1996, 54, 10175-10185.	3.2	36
221	Magnetically recyclable Fe@Co core-shell catalysts for dehydrogenation of sodium borohydride in fuel cells. International Journal of Hydrogen Energy, 2012, 37, 3338-3343.	7.1	36
222	Chitosan-Modified Stable Colloidal Gold Nanostars for the Photothermolysis of Cancer Cells. Journal of Physical Chemistry C, 2013, 117, 2396-2410.	3.1	36
223	Hole concentration in the three-CuO2-plane copper-oxide superconductor Cu-1223. Journal of Solid State Chemistry, 2004, 177, 1037-1043.	2.9	35
224	Using binary resistors to achieve multilevel resistive switching in multilayer NiO/Pt nanowire arrays. NPG Asia Materials, 2014, 6, e85-e85.	7.9	35
225	Comparative Study of Li–CO ₂ and Na–CO ₂ Batteries with Ru@CNT as a Cathode Catalyst. ACS Applied Materials & Interfaces, 2021, 13, 480-490.	8.0	35
226	Superconductivity up to 32 K in a new family of the Hg-containing (Pb, Hg) (Sr, La)2CuO5â^1^´ (1201) system. Physica C: Superconductivity and Its Applications, 1993, 216, 237-242.	1.2	34
227	Neutron diffraction study, magnetic properties and thermal stability of YMn2D6 synthesized under high deuterium pressure. Journal of Solid State Chemistry, 2005, 178, 356-362.	2.9	34
228	Effects of B′-site transition metal on the properties of double perovskites Sr2FeMO6 (M=Mo, W): B′ 4d–5d system. Solid State Communications, 2005, 133, 265-270.	1.9	34
229	High specific capacity retention of graphene/silicon nanosized sandwich structure fabricated by continuous electron beam evaporation as anode for lithium-ion batteries. Electrochimica Acta, 2015, 165, 166-172.	5.2	34
230	Broadband near-infrared persistent luminescence of Ba[Mg ₂ Al ₂ N ₄] with Eu ²⁺ and Tm ³⁺ after red light charging. Journal of Materials Chemistry C, 2019, 7, 1705-1712.	5.5	34
231	Nextâ€Generation Cancerâ€5pecific Hybrid Theranostic Nanomaterials: MAGEâ€A3 NIR Persistent Luminescence Nanoparticles Conjugated to Afatinib for In Situ Suppression of Lung Adenocarcinoma Growth and Metastasis. Advanced Science, 2020, 7, 1903741.	11.2	34
232	Improvement in quantum yield by suppression of trions in room temperature synthesized CsPbBr ₃ perovskite quantum dots for backlight displays. Nanoscale, 2020, 12, 3820-3826.	5.6	34
233	Crystal Structures and Peculiar Magnetic Properties of α- and γ-Al2O3 Powders. Modern Physics Letters B, 1997, 11, 1169-1174.	1.9	33
234	Synthesis, electrochemical properties, and characterization of LiFePO4/C composite by a two-source method. Journal of Alloys and Compounds, 2009, 487, 58-63.	5.5	33

#	Article	IF	CITATIONS
235	Pdâ^'Câ^'Fe Nanoparticles Investigated by X-ray Absorption Spectroscopy as Electrocatalysts for Oxygen Reduction. Chemistry of Materials, 2009, 21, 4030-4036.	6.7	33
236	Energy Transfer and Significant Improvement Moist Stability of BaMgAl[sub 10]O[sub 17]:Eu[sup 2+],Mn[sup 2+] as a Phosphor for White Light-Emitting Diodes. Journal of the Electrochemical Society, 2010, 157, J307.	2.9	33
237	Ag–Si artificial microflowers for plasmon-enhanced solar water splitting. Chemical Communications, 2015, 51, 549-552.	4.1	33
238	Temperature effect on the emission spectra of narrow band Mn ⁴⁺ phosphors for application in LEDs. Physical Chemistry Chemical Physics, 2017, 19, 32505-32513.	2.8	33
239	Alcohol-Guided Growth of Two-Dimensional Narrow-Band Red-Emitting K ₂ TiF ₆ :Mn ⁴⁺ for White-Light-Emitting Diodes. ACS Applied Materials & Interfaces, 2019, 11, 20143-20149.	8.0	33
240	Microfluidic synthesis of CsPbBr3/Cs4PbBr6 nanocrystals for inkjet printing of mini-LEDs. Chemical Engineering Journal, 2021, 426, 130849.	12.7	33
241	The Great Flexibility of the Rock Salt Layers in the Lead-Based 1212 High-Tc Superconductive Cuprates: The Oxides (Pb, A)Sr2(Ca, Ln)Cu2O7-δ. Journal of Solid State Chemistry, 1993, 102, 31-39.	2.9	32
242	Layer-specific hole concentrations inBi2Sr2(Y1â^'xCax)Cu2O8+l´as probed by XANES spectroscopy and coulometric redox analysis. Physical Review B, 2003, 67, .	3.2	32
243	Valence State of Iron in the Sr2Fe(Mo,W,Ta)O6.0Double-Perovskite System:Â an FeK-edge andL2,3-edge XANES Study. Chemistry of Materials, 2003, 15, 4118-4121.	6.7	32
244	Influence of pyrolysis temperature on oxygen reduction reaction activity of carbon-incorporating iron nitride/nitrogen-doped graphene nanosheets catalyst. International Journal of Hydrogen Energy, 2013, 38, 3956-3962.	7.1	32
245	All-In-One Light-Tunable Borated Phosphors with Chemical and Luminescence Dynamical Control Resolution. ACS Applied Materials & Interfaces, 2014, 6, 9160-9172.	8.0	32
246	Quantum-Dot-Sensitized Nitrogen-Doped ZnO for Efficient Photoelectrochemical Water Splitting. European Journal of Inorganic Chemistry, 2014, 2014, 773-779.	2.0	31
247	(INVITED) Recent progress on broadband near-infrared phosphors-converted light emitting diodes for future miniature spectrometers. Optical Materials: X, 2019, 1, 100011.	0.8	31
248	Nearâ€Infrared Nanophosphor Embedded in Mesoporous Silica Nanoparticle with High Lightâ€Harvesting Efficiency for Dual Photosystem Enhancement. Angewandte Chemie - International Edition, 2021, 60, 6955-6959.	13.8	31
249	High-Performance NaK ₂ Li[Li ₃ SiO ₄] ₄ :Eu Green Phosphor for Backlighting Light-Emitting Diodes. Chemistry of Materials, 2021, 33, 1893-1899.	6.7	31
250	Improvement of phase purity and accelerated formation of the Tl-1223 phase from the stoichiometric compositions (Tl0.6Pb0.2Bi0.2) (Sr2-xBax)Ca2Cu3O9 (x=0.2-0.3). Physica C: Superconductivity and Its Applications, 1994, 222, 278-282.	1.2	30
251	Determination of Mn Valence from X-Ray Absorption Near Edge Structure and Study of Magnetic Behavior in Hole-Doped (Nd1â^'xCax)MnO3System. Journal of Solid State Chemistry, 1996, 125, 112-115.	2.9	30
252	The novel YMn2D6 deuteride synthesized under high pressure of gaseous deuterium. Solid State Communications, 2004, 130, 815-820.	1.9	30

#	Article	IF	CITATIONS
253	Highly Luminescent CsPbBr ₃ @Cs ₄ PbBr ₆ Nanocrystals and Their Application in Electroluminescent Emitters. Journal of Physical Chemistry Letters, 2020, 11, 10196-10202.	4.6	30
254	Integrated therapy platform of exosomal system: hybrid inorganic/organic nanoparticles with exosomes for cancer treatment. Nanoscale Horizons, 2022, 7, 352-367.	8.0	30
255	Crystal and electronic structures of inverse spinel-type LiNiVO4. Materials Research Bulletin, 2001, 36, 1479-1486.	5.2	29
256	In Situ and Ex Situ Monitoring of Oxygen Absorption in YBaCo4O7+δ. Chemistry Letters, 2007, 36, 1368-1369.	1.3	29
257	Biocompatible transferrin-conjugated sodium hexametaphosphate-stabilized gold nanoparticles: synthesis, characterization, cytotoxicity and cellular uptake. Nanotechnology, 2011, 22, 395706.	2.6	29
258	Pressure effect on the zero-phonon line emission of Mn4+ in K2SiF6. Journal of Chemical Physics, 2015, 143, 134704.	3.0	29
259	Magnetically Guided Theranostics: Optimizing Magnetic Resonance Imaging with Sandwich-Like Kaolinite-Based Iron/Platinum Nanoparticles for Magnetic Fluid Hyperthermia and Chemotherapy. Chemistry of Materials, 2020, 32, 697-708.	6.7	29
260	Efficient Luminescence from CsPbBr ₃ Nanoparticles Embedded in Cs ₄ PbBr ₆ . Journal of Physical Chemistry Letters, 2020, 11, 7637-7642.	4.6	29
261	Improvement of lithium anode deterioration for ameliorating cyclabilities of non-aqueous Li–CO ₂ batteries. Nanoscale, 2020, 12, 8385-8396.	5.6	29
262	Na–CO2 battery with NASICON-structured solid-state electrolyte. Nano Energy, 2021, 85, 105972.	16.0	29
263	Crystal structure of the (Pb, Hg)Sr2(Ca, Y)Cu2O7-δ superconductor. Physica C: Superconductivity and Its Applications, 1994, 222, 13-18.	1.2	28
264	Ce K-edge EXAFS study of nanocrystalline CeO2. Materials Research Bulletin, 2002, 37, 555-562.	5.2	28
265	Magnetocaloric effect and magnetic properties of Tb0.9Sn0.1MnO3. Journal of Applied Physics, 2007, 101, 103904.	2.5	28
266	Structural Transformation of LiVOPO ₄ to Li ₃ V ₂ (PO ₄) ₃ with Enhanced Capacity. Journal of Physical Chemistry B, 2008, 112, 11250-11257.	2.6	28
267	The fabrication and characterization of superconducting Tl-Pb-Ca-Pr-Sr-Cu-O compounds with Y1Ba2Cu3Oy-like structure and Tc (zero) up to 106 K. Physica C: Superconductivity and Its Applications, 1989, 159, 385-390.	1.2	27
268	Superconductivity at 133 K in Tl2Ba2Ca2Cu3O10+x under high pressure. Physica C: Superconductivity and Its Applications, 1993, 218, 24-28.	1.2	27
269	Pressure effects on the transport and magnetic properties ofLa1.4Sr1.6Mn2O7. Physical Review B, 1998, 58, 12224-12229.	3.2	27
270	Investigation on Mechanism of Catalysis by Ptâ^'LiCoO ₂ for Hydrolysis of Sodium Borohydride Using X-ray Absorption. Journal of Physical Chemistry B, 2008, 112, 4870-4875.	2.6	27

#	Article	IF	CITATIONS
271	Amorphous Phosphorus-Doped Cobalt Sulfide Modified on Silicon Pyramids for Efficient Solar Water Reduction. ACS Applied Materials & Interfaces, 2018, 10, 37142-37149.	8.0	27
272	Natural Carbon Nanodots: Toxicity Assessment and Theranostic Biological Application. Pharmaceutics, 2021, 13, 1874.	4.5	27
273	Structural, electrical and magnetic properties of two-dimensional La1.2(Sr1.8â^`xCax)Mn2O7 manganites. Journal of Applied Physics, 1999, 86, 2178-2184.	2.5	26
274	Chemical Size Effect on the Magnetic and Electrical Properties in the (Tb1-xEux)MnO3(0 â‰ ¤ ≤1.0) System. Journal of Physical Chemistry B, 2007, 111, 2262-2267.	2.6	26
275	Improvement of resistive switching in NiO-based nanowires by inserting Pt layers. Applied Physics Letters, 2012, 101, .	3.3	26
276	Inorganic red perovskite quantum dot integrated blue chip: a promising candidate for high color-rendering in w-LEDs. RSC Advances, 2016, 6, 79410-79414.	3.6	26
277	Disentangling Red Emission and Compensatory Defects in Sr[LiAl ₃ N ₄]:Ce ³⁺ Phosphor. Chemistry of Materials, 2018, 30, 4493-4497.	6.7	26
278	Photo-/electro-luminescence enhancement of CsPbX ₃ (X = Cl, Br, or I) perovskite quantum dots <i>via</i> thiocyanate surface modification. Journal of Materials Chemistry C, 2020, 8, 1065-1071.	5.5	26
279	Synthesis and characterization for a new family of Tl-containing septenary oxides with Tc,zero above 105 K. Physica C: Superconductivity and Its Applications, 1989, 162-164, 869-870.	1.2	25
280	Chemical Tuning of Structure, Magnetization, and Conductivity in the Self-doped Double-Perovskite (Sr2-xCax)FeMoO6(0 â‰ඤෲරීයාව, System. Chemistry of Materials, 2003, 15, 425-432.	6.7	25
281	Local structural characterization of Au/Pt bimetallic nanoparticles. Chemical Physics Letters, 2006, 420, 484-488.	2.6	25
282	Carbon incorporated FeN/C electrocatalyst for oxygen reduction enhancement in direct methanol fuel cells: X-ray absorption approach to local structures. Electrochimica Acta, 2011, 56, 8734-8738.	5.2	25
283	Pressure-controlled synthesis of high-performance SrLiAl ₃ N ₄ :Eu ²⁺ narrow-band red phosphors. Journal of Materials Chemistry C, 2018, 6, 10174-10178.	5.5	25
284	High-performance Na–CO ₂ batteries with ZnCo ₂ O ₄ @CNT as the cathode catalyst. Journal of Materials Chemistry A, 2020, 8, 23974-23982.	10.3	25
285	Effect of Temperature and Pressure on Structural and Optical Properties of Organic–Inorganic Hybrid Manganese Halides. Inorganic Chemistry, 2022, 61, 2595-2602.	4.0	25
286	Preparation of HIGH-Jc superconducting oxide in the Bi-Sr-Ca-Cu-O system by oxalate gel processing. Materials Letters, 1989, 8, 228-232.	2.6	24
287	First example of indium as a practical alternative to thallium in high-Tc superconductors. Physica C: Superconductivity and Its Applications, 1990, 165, 111-114.	1.2	24
288	Magnetic instability and oxygen deficiency in Na-dopedTbMnO3. Physical Review B, 2006, 74, .	3.2	24

#	Article	IF	CITATIONS
289	Melilite-type blue chromophores based on Mn3+ in a trigonal-bipyramidal coordination induced by interstitial oxygen. Journal of Materials Chemistry C, 2013, 1, 5843.	5.5	24
290	A heteroelectrode structure for solar water splitting: integrated cobalt ditelluride across a TiO ₂ -passivated silicon microwire array. Catalysis Science and Technology, 2017, 7, 1488-1496.	4.1	24
291	Plasmonâ€Enhanced Electrocatalytic Properties of Rationally Designed Hybrid Nanostructures at a Catalytic Interface. Advanced Materials Interfaces, 2019, 6, 1801144.	3.7	24
292	Curtailing the Overpotential of Li–CO 2 Batteries with Shapeâ€Controlled Cu 2 O as Cathode: Effect of Illuminating the Cathode. ChemSusChem, 2020, 13, 2719-2725.	6.8	24
293	Enticing applications of <scp>nearâ€infrared</scp> phosphors: Review and future perspectives. Journal of the Chinese Chemical Society, 2021, 68, 206-215.	1.4	24
294	Effective Ru/CNT Cathode for Rechargeable Solid-State Li–CO ₂ Batteries. ACS Applied Materials & Interfaces, 2021, 13, 44266-44273.	8.0	24
295	Structural, electrical and magnetic characterization of the double perovskites Sr2CrMO6 (M=Mo, W): B′ 4d–5d system. Solid State Communications, 2004, 131, 531-535.	1.9	23
296	Anode catalysts for enhanced methanol oxidation: An in situ XANES study of PtRu/C and PtMo/C catalysts. Chemical Physics Letters, 2005, 412, 444-448.	2.6	23
297	Electrodeposition of nano-dimensioned FeSe. Thin Solid Films, 2011, 519, 8397-8400.	1.8	23
298	Thermal effects in (oxy)nitride phosphors. Journal of Solid State Lighting, 2014, 1, .	2.3	23
299	Domination of Second-Sphere Shrinkage Effect To Improve Photoluminescence of Red Nitride Phosphors. Inorganic Chemistry, 2014, 53, 12822-12831.	4.0	23
300	Biogenic Reduction of Graphene Oxide: An Efficient Superparamagnetic Material for Photocatalytic Hydrogen Production. ACS Applied Energy Materials, 2018, 1, 5907-5918.	5.1	23
301	Molybdenum Tungsten Disulfide with a Large Number of Sulfur Vacancies and Electronic Unoccupied States on Silicon Micropillars for Solar Hydrogen Evolution. ACS Applied Materials & Interfaces, 2020, 12, 54671-54682.	8.0	23
302	ZnSe:Te/ZnSeS/ZnS nanocrystals: an access to cadmium-free pure-blue quantum-dot light-emitting diodes. Nanoscale, 2020, 12, 11556-11561.	5.6	23
303	Epitaxial growth of high Tc superconducting Yâ€Baâ€Cuâ€O thin films on (001)MgO by a chemical spray pyrolysis method. Journal of Applied Physics, 1988, 64, 2523-2526.	2.5	22
304	Preparation and characterization of superconducting bismuth lead strontium calcium copper oxides[(Bi,Pb)2Sr2Ca2Cu3] oxides with Tc above 110 K by coprecipitation in triethylamine media. Inorganic Chemistry, 1990, 29, 3117-3119.	4.0	22
305	The synthesis, by triethylammoniumoxalate coprecipitation, and superconducting properties of Y(Ba1â^xSrx)2Cu4O8. Journal of Solid State Chemistry, 1991, 92, 247-252.	2.9	22
306	Cr doping in the La1.2Sr1.8Mn2O7system. Journal of Physics Condensed Matter, 1999, 11, 5187-5194.	1.8	22

#	Article	IF	CITATIONS
307	Phase stability study of La1.2Ca1.8Mn2O7. Materials Research Bulletin, 2001, 36, 1139-1148.	5.2	22
308	Hydrides of Laves phases intermetallic compounds synthesized under high hydrogen pressure. Solid State Ionics, 2010, 181, 306-310.	2.7	22
309	Sulfonation of graphene nanosheet-supported platinum via a simple thermal-treatment toward its oxygen reduction activity in acid medium. International Journal of Hydrogen Energy, 2012, 37, 14205-14210.	7.1	22
310	Wide Range pH-Tolerable Silicon@Pyrite Cobalt Dichalcogenide Microwire Array Photoelectrodes for Solar Hydrogen Evolution. ACS Applied Materials & amp; Interfaces, 2016, 8, 5400-5407.	8.0	22
311	Matchmaker of Marriage between a Li Metal Anode and NASICON-Structured Solid-State Electrolyte: Plastic Crystal Electrolyte and Three-Dimensional Host Structure. ACS Applied Materials & Interfaces, 2020, 12, 44754-44761.	8.0	22
312	Ultra-broadband near-infrared emission CuInS ₂ /ZnS quantum dots with high power efficiency and stability for the theranostic applications of mini light-emitting diodes. Chemical Communications, 2020, 56, 8285-8288.	4.1	22
313	Combinatorial Search for Green and Blue Phosphors of High Thermal Stabilities under UV Excitation Based on the K(Sr1â^'xâ^'y)PO4:Tb3+xEu2+y System. ACS Combinatorial Science, 2008, 10, 847-850.	3.3	21
314	Photoluminescent and Thermal Stable Properties of Tb[sup 3+]-Doped Ca-α-SiAlON under VUV Excitation. Journal of the Electrochemical Society, 2009, 156, J189.	2.9	21
315	High-resolution X-ray absorption near edge structure studies of monophasic Tl2Ba2Ca2Cu3O10â^î^ (Tl-2223) superconductor. Solid State Communications, 1996, 99, 493-498.	1.9	20
316	Hole distribution in (Tl0.5Pb0.5)Sr2(Ca1â^'xYx)Cu2O7studied by x-ray absorption spectroscopy. Physical Review B, 1996, 54, 12587-12593.	3.2	20
317	Pressure dependence of the superconducting critical temperature of the TIO.5Pb0.5Sr2Ca1â^xYxCu2O7system. Physical Review B, 1997, 55, 11832-11838.	3.2	20
318	Hole doping in Pb-free and Pb-substituted(Bi,Pb)2Sr2Ca2Cu3O10+δsuperconductors. Physical Review B, 2003, 68, .	3.2	20
319	Pb-for-Bi substitution for enhancing thermoelectric characteristics of [(Bi,Pb)2Ba2O4±ï‰]0.5CoO2. Applied Physics Letters, 2006, 88, 232102.	3.3	20
320	Luminescent Properties and Structure Investigation of Y[sub 3]Al[sub 5]O[sub 12]â^•Ce Phosphors with Si Addition. Journal of the Electrochemical Society, 2007, 154, P16.	2.9	20
321	The effect of terbium concentration on the luminescent properties of yttrium oxysulfide phosphor for FED application. Journal of Luminescence, 2007, 122-123, 574-576.	3.1	20
322	Strong orbital polarization in orthorhombic <mml:math xmlns:mml="http://www.w3.org/1998/Math/MathML" display="inline"><mml:mrow><mml:msub><mml:mrow><mml:mtext>DyMnO</mml:mtext></mml:mrow><mml: A combined x-ray linear dichroism and<i>ab initio</i>electronic structure study. Physical Review B,</mml: </mml:msub></mml:mrow></mml:math 	:m ቴኦ ୫ <td>.ml20n></td>	.ml 20 n>
323	2010, 81, Luminescence Spectra of β-SiAlON/Pr3+ Under High Hydrostatic Pressure. Journal of Physical Chemistry C, 2013, 117, 13181-13186.	3.1	20
324	Cobalt Diselenide Nanorods Grafted on Graphitic Carbon Nitride: A Synergistic Catalyst for Oxygen Reactions in Rechargeable Liâ~'O ₂ Batteries. ChemElectroChem, 2018, 5, 29-35.	3.4	20

#	Article	IF	CITATIONS
325	Gelatin sponge functionalized with gold/silver clusters for antibacterial application. Nanotechnology, 2020, 31, 134004.	2.6	20
326	Chemical and Mechanical Pressure-Induced Photoluminescence Tuning via Structural Evolution and Hydrostatic Pressure. Chemistry of Materials, 2021, 33, 3832-3840.	6.7	20
327	63Cu NMR shift and relaxation behavior in Tl2Ba2Ca2Cu3O10â^î´ (Tc=125K). Physica C: Superconductivity and Its Applications, 1994, 226, 106-112.	1.2	19
328	Effect of Co ₂ P on Electrochemical Performance of Li(Mn _{0.35} Co _{0.2} Fe _{0.45})PO ₄ /C. Journal of Physical Chemistry B, 2008, 112, 8017-8023.	2.6	19
329	Highly Efficient Photoelectrochemical Hydrogen Generation Reaction Using Tungsten Phosphosulfide Nanosheets. ACS Applied Materials & Interfaces, 2018, 10, 17280-17286.	8.0	19
330	Reconstruction of Mn4+-free shell achieving highly stable red-emitting fluoride phosphors for light-emitting diodes. Chemical Engineering Journal, 2021, 426, 131350.	12.7	19
331	Plasmon-Triggered Upconversion Emissions and Hot Carrier Injection for Combinatorial Photothermal and Photodynamic Cancer Therapy. ACS Applied Materials & Interfaces, 2021, 13, 58422-58433.	8.0	19
332	The optical research progress of nanophosphors composed of transition elements in the fourth period of near-infrared windows I and II for deep-tissue theranostics. Nanoscale, 2022, 14, 7123-7136.	5.6	19
333	A new high-Tc superconducting Tl-Pb-Ca-Sr-Cu-O system. Physica C: Superconductivity and Its Applications, 1988, 156, 791-794.	1.2	18
334	Absence of oxygen stoichiometry effects on Tc in a Tl-1122 superconductor. Physica C: Superconductivity and Its Applications, 1989, 161, 523-526.	1.2	18
335	Crystal and electronic structures of (Ba, Sr)TiO3. Materials Letters, 1998, 37, 285-289.	2.6	18
336	A comparison of the properties of Bi-2223 precursor powders synthesized by various methods. Materials Research Bulletin, 2001, 36, 1653-1658.	5.2	18
337	Electronic Structures, Hole-Doping, and Superconductivity of the s = 1, 2, 3, and 4 Members of the (Cu,Mo)-12s2 Homologous Series of Superconductive Copper Oxides. Journal of the American Chemical Society, 2010, 132, 838-841.	13.7	18
338	An intelligent approach to the discovery of luminescent materials using a combinatorial approach combined with Taguchi methodology. Luminescence, 2011, 26, 229-238.	2.9	18
339	Catalytically Active Site Identification of Molybdenum Disulfide as Gas Cathode in a Nonaqueous Li–CO ₂ Battery. ACS Applied Materials & Interfaces, 2021, 13, 6156-6167.	8.0	18
340	Structural characterization of a TlCaBaCu oxide inTconset=155 K andTczero=123 K superconducting specimens. Applied Physics Letters, 1988, 53, 1434-1436.	3.3	17
341	Soft-x-ray absorption spectroscopy ofNd1+xBa2â~'xCu3O7+Î′s(x=0–0.6). Physical Review B, 1997, 55, 3186-3191.	3.2	17
342	Electronic and Local Structural Properties of the Bi2Sr2(Ca1-xYx)Cu2O8+Î′ Family of Materials, Studied by X-ray Absorption Spectroscopy. Chemistry of Materials, 2000, 12, 1115-1121.	6.7	17

#	Article	IF	CITATIONS
343	Oxygen Content and Valence of Ru in RuSr2(Gd0.75Ce0.25)2Cu2O10â [~] ´î´ (Ru-1222) Magnetosuperconductor. Journal of Low Temperature Physics, 2003, 131, 1211-1216.	1.4	17
344	Oxygen non-stoichiometry in Ru-1212 and Ru-1222 magnetosuperconductors. Physica C: Superconductivity and Its Applications, 2003, 392-396, 87-92.	1.2	17
345	Structure and physical properties of double perovskite compounds Sr2FeMO6 (M=Mo, W). Materials Chemistry and Physics, 2005, 93, 314-319.	4.0	17
346	Intense X-ray induced formation of silver nanoparticles stabilized byÂbiocompatible polymers. Applied Physics A: Materials Science and Processing, 2009, 97, 295-300.	2.3	17
347	Mechanism of light emission and electronic properties of a Eu3+-doped Bi2SrTa2O9 system determined by coupled X-ray absorption and emission spectroscopy. Journal of Materials Chemistry, 2011, 21, 17119.	6.7	17
348	Luminescence and density functional theory (DFT) calculation of undoped nitridosilicate phosphors for light-emitting diodes. Journal of Materials Chemistry, 2012, 22, 5828.	6.7	17
349	Monitoring the phase evolution in LiCoO ₂ electrodes during battery cycles using inâ€situ neutron diffraction technique. Journal of the Chinese Chemical Society, 2020, 67, 344-352.	1.4	17
350	Disorder–Order Conversionâ€Induced Enhancement of Thermal Stability of Pyroxene Nearâ€Infrared Phosphors for Lightâ€Emitting Diodes. Angewandte Chemie, 2022, 134, .	2.0	17
351	In Situ Growth of High-Quality CsPbBr ₃ Quantum Dots with Unusual Morphology inside a Transparent Glass with a Heterogeneous Crystallization Environment for Wide Gamut Displays. ACS Applied Materials & Interfaces, 2022, 14, 30029-30038.	8.0	17
352	Bonding anisotropy in multiferroic TbMnO3 probed by polarization dependent x-ray absorption spectroscopy. Applied Physics Letters, 2009, 94, .	3.3	16
353	The temperatureâ€sensitive luminescence of (Y,Gd)VO ₄ :Bi ³⁺ ,Eu ³⁺ and its application for stealth antiâ€counterfeiting. Physica Status Solidi - Rapid Research Letters, 2012, 6, 321-323.	2.4	16
354	Rutile-type (Ti,Sn)O2 nanorods as efficient anode materials toward its lithium storage capabilities. Nanoscale, 2013, 5, 2254.	5.6	16
355	Quantum dots for light conversion, therapeutic and energy storage applications. Journal of Solid State Chemistry, 2019, 270, 71-84.	2.9	16
356	Hydrogen-Containing Na3HTi1–xMnxF8 Narrow-Band Phosphor for Light-Emitting Diodes. ACS Energy Letters, 2019, 4, 527-533.	17.4	16
357	<i>In situ</i> synthesis of high-efficiency CsPbBr ₃ /CsPb ₂ Br ₅ composite nanocrystals in aqueous solution of microemulsion. Green Chemistry, 2020, 22, 5257-5261.	9.0	16
358	Correlations between bond lengths,Tc, and O vibration frequencies: Raman-scattering and infrared-absorption study of the 1:2:1:2 structure (Ca1â^'yYy)Sr2(Tl0.5Pb0.5)Cu2O7as a function of doping. Physical Review B, 1993, 47, 12104-12109.	3.2	15
359	Origin of superconductivity suppression in (Dy1â°'xPrx)Ba2Cu3O7studied by soft-x-ray absorption spectroscopy. Physical Review B, 1997, 55, 14586-14591.	3.2	15
360	Synthesis and characterization of the colossal magnetoresistance manganite La1.2(Sr1.4Ca0.4)Mn2O7 by citrate gel. Materials Research Bulletin, 2002, 37, 235-246.	5.2	15

#	Article	IF	CITATIONS
361	XANES Study on the Generation and Distribution of Holes via Ca Substitution and O Doping in Cu(Ba0.8Sr0.2)2(Yb1â^'xCax)Cu2O6+z. Journal of Solid State Chemistry, 2002, 166, 229-236.	2.9	15
362	Crystalline and magnetic structures of Sr2FeMoO6 double perovskites. Physica B: Condensed Matter, 2006, 385-386, 418-420.	2.7	15
363	Mössbauer study on LiFePO4 cathode material for lithium ion batteries. Hyperfine Interactions, 2006, 167, 767-772.	0.5	15
364	energy transfer in (,) doped with. Radiation Measurements, 2007, 42, 755-758.	1.4	15
365	Advances in Carbonâ€Incorporated Nonâ€Noble Transition Metal Catalysts for Oxygen Reduction Reaction in Polymer Electrolyte Fuel Cells. Journal of the Chinese Chemical Society, 2014, 61, 93-100.	1.4	15
366	Capacity Enhancement of the Quenched Li-Ni-Mn-Co Oxide High-voltage Li-ion Battery Positive Electrode. Electrochimica Acta, 2017, 236, 10-17.	5.2	15
367	Nano-lipospheres as acoustically active ultrasound contrast agents: evolving tumor imaging and therapy technique. Nanotechnology, 2019, 30, 182001.	2.6	15
368	Synthesis, transport, magnetization and structural characterizations of Tl-Ca-Ba-Cu-O specimens with TO=123 K and Tonset=155 K. Physica C: Superconductivity and Its Applications, 1988, 156, 109-112.	1.2	14
369	X-ray absorption near edge structure studies of colossal magnetoresistance ferromagnet (La1.4Sr1.6)Mn2O7. Solid State Communications, 1998, 105, 605-608.	1.9	14
370	Absence of phase transformation at low temperature in Co-doped LiMn2O4 samples. Dalton Transactions RSC, 2001, , 37-40.	2.3	14
371	A Novel Anode Material LiVMoO[sub 6] for Rechargeable Lithium-Ion Batteries. Electrochemical and Solid-State Letters, 2005, 8, A650.	2.2	14
372	energy transfer in Ce3+-doped Y3â^'xTbxGd0.65Al5O12. Journal of Physics Condensed Matter, 2006, 18, 10531-10543.	1.8	14
373	Vacuum Ultraviolet Excitable Mn[sup 2+]-Doped LiZnPO[sub 4] Phosphors for PDP Applications. Journal of the Electrochemical Society, 2008, 155, J284.	2.9	14
374	Spiralâ€Type Heteropolyhedral Coordination Network Based on Singleâ€Crystal LiSrPO ₄ : Implications for Luminescent Materials. Chemistry - A European Journal, 2013, 19, 15358-15365.	3.3	14
375	Evaluation of the intracellular uptake and cytotoxicity effect of TiO ₂ nanostructures for various human oral and lung cells under dark conditions. Toxicology Research, 2016, 5, 303-311.	2.1	14
376	An insight into the preferential substitution and structure repair in Eu ²⁺ -doped whitlockite-type phosphors based on the combined experimental and theoretical calculations. Journal of Materials Chemistry C, 2019, 7, 8954-8961.	5.5	14
377	Broadband NaK ₂ Li[Li ₃ SiO ₄] ₄ :Ce Alkali Lithosilicate Blue Phosphors. Journal of Physical Chemistry Letters, 2020, 11, 6621-6625.	4.6	14
378	Singleâ€Crystal Red Phosphors and Their Core–Shell Structure for Improved Waterâ€Resistance for Laser Diodes Applications. Angewandte Chemie, 2021, 133, 3986-3991.	2.0	14

#	Article	IF	CITATIONS
379	Comprehensive view on recent developments in hydrogen evolution using MoS ₂ on a Si photocathode: from electronic to electrochemical aspects. Journal of Materials Chemistry A, 2021, 9, 3767-3785.	10.3	14
380	Photoluminescence enhancement study in a Bi-doped Cs ₂ AgInCl ₆ double perovskite by pressure and temperature-dependent self-trapped exciton emission. Dalton Transactions, 2022, 51, 2026-2032.	3.3	14
381	<i>M</i> _{<i>x</i>} La _{1–<i>x</i>} SiO _{2–<i>y</i>} N _{<i>z</i>} (<i>M</i> = Ca/Sr/Ba): Elucidating and Tuning the Structure and Eu ²⁺ Local Environments to Develop Full-Visible Spectrum Phosphors. Chemistry of Materials, 2022, 34, 4039-4049.	6.7	14
382	Bulk superconductivity withTc(zero) up to 95 K in a Tl0.5Pb0.5Ca0.9Ce0.1Sr2Cu2oxide with an Y1Ba2Cu3Oyâ€like structure. Applied Physics Letters, 1989, 54, 2464-2466.	3.3	13
383	Evidence for electron-doped (n-type) superconductivity in the infinite-layer (Sr0.9La0.1)CuO2 compound by X-ray absorption near-edge spectroscopy. Solid State Communications, 2001, 118, 367-370.	1.9	13
384	Charge transport mechanism in LiCoyMn2â [^] yO4 cathode material. Solid State Ionics, 2003, 157, 101-108.	2.7	13
385	Direct White Light Phosphor Based on Metallorganic Coordination Extended Networks for UV-Light-Emitting Diodes. Journal of the Electrochemical Society, 2008, 155, P71.	2.9	13
386	Spectroscopic properties and energy level location of Eu2+ in Sr2Si5N8 phosphor. Optical Materials, 2014, 37, 734-739.	3.6	13
387	Improvement of the Water Resistance of a Narrowâ€Band Redâ€Emitting SrLiAl ₃ N ₄ :Eu ²⁺ Phosphor Synthesized under High Isostatic Pressure through Coating with an Organosilica Layer. Angewandte Chemie, 2016, 128, 9804-9808.	2.0	13
388	Structural phase transitions and photoluminescence properties of oxonitridosilicate phosphors under high hydrostatic pressure. Scientific Reports, 2016, 6, 34010.	3.3	13
389	Synthesis of ultra-stable perovskite composite quantum dots for light-emitting diodes. Green Chemistry, 2021, 23, 8871-8877.	9.0	13
390	Extensively Reducing Interfacial Resistance by the Ultrathin Pt Layer between the Garnet-Type Solid-State Electrolyte and Li–Metal Anode. ACS Applied Materials & Interfaces, 2021, 13, 56181-56190.	8.0	13
391	Correlated Na ⁺ Ion Migration Invokes Zero Thermal Quenching in a Sodium Superionic Conductor-type Phosphor. Chemistry of Materials, 2022, 34, 107-115.	6.7	13
392	Hole states in fluorine-dopedLa2CuO4thin films probed by polarized x-ray-absorption spectroscopy. Physical Review B, 1999, 60, 6888-6892.	3.2	12
393	Structural, thermal and magnetic properties of ErMn2D6synthesized under high deuterium pressure. Journal of Physics Condensed Matter, 2006, 18, 6409-6420.	1.8	12
394	Resonant x-ray emission spectroscopy of multiferroic TbMnO3. Applied Physics Letters, 2007, 91, .	3.3	12
395	Charge compensation and oxidation in NaxCoO2â^î^ and LixCoO2â^î^ studied by XANES. Journal of Solid State Chemistry, 2007, 180, 1608-1615.	2.9	12
396	Band overlap via chemical pressure control in double perovskite (Sr2â^'xCax)FeMoO6 (0⩼2x⩽2.0) with TN effect. Current Applied Physics, 2008, 8, 110-113.	1R _{2.4}	12

#	Article	IF	CITATIONS
397	A rare earth-free GaZnON phosphor prepared by combustion for white light-emitting diodes. Journal of Materials Chemistry C, 2015, 3, 1473-1479.	5.5	12
398	Long-Term Near-Infrared Signal Tracking of the Therapeutic Changes of Glioblastoma Cells in Brain Tissue with Ultrasound-Guided Persistent Luminescent Nanocomposites. ACS Applied Materials & Interfaces, 2021, 13, 6099-6108.	8.0	12
399	Revealing the absence of carbon in aprotic Li–CO ₂ batteries: a mechanism study toward CO ₂ reduction under a pure CO ₂ environment. Journal of Materials Chemistry A, 2022, 10, 3460-3468.	10.3	12
400	Superconductivity of Y1Ba2â^'xSrxCu3Oy system. Physica C: Superconductivity and Its Applications, 1988, 153-155, 866-867.	1.2	11
401	Zero resistance up to 162 K in a multiphase Tl-Ca-Ba-Cu-O system. Physical Review B, 1989, 39, 2792-2795.	3.2	11
402	Crystal Structure and Superconductivity of the Mo-Stabilized Sr-Based YSr2Cu2.7Mo0.3O7-δCompound. Journal of Solid State Chemistry, 1994, 112, 203-207.	2.9	11
403	Hole Distribution in Underdoped and Overdoped Y(Ba2-ySry)Cu3O6+δCompounds Studied by X-ray Absorption Spectroscopy. Inorganic Chemistry, 1998, 37, 5527-5531.	4.0	11
404	Superconductivity suppression ofR(Ba1â^'zRz)2Cu3O7+δ(R=Nd,Pr) probed by soft-x-ray absorption spectroscopy. Physical Review B, 1999, 59, 3855-3861.	3.2	11
405	Hole doping and superconductivity characteristics of the s=1, 2 and 3 members of the (Cu,Mo)-12s2 homologous series of layered copper oxides. Journal of Solid State Chemistry, 2005, 178, 3464-3470.	2.9	11
406	Electron-doping through Lalll-for-SrII substitution in (Sr1â^'xLax)2FeTaO6: Effects on the valences and ordering of the B-site cations, Fe and Ta. Journal of Solid State Chemistry, 2006, 179, 111-116.	2.9	11
407	Zeolitic imidazolate framework [Zn2(IM)4·(DMF)] for UV-white light-emitting diodes. Dalton Transactions, 2012, 41, 11885.	3.3	11
408	Electrochemical reduction of high-efficiency ozone generation through nitrogen-doped diamond-like carbon electrodes. RSC Advances, 2013, 3, 5917.	3.6	11
409	New Pr3+ site in β-SiAlON red phosphor. Optical Materials, 2013, 35, 2001-2005.	3.6	11
410	Broadband Cr ³⁺ , Sn ⁴⁺ â€Doped Oxide Nanophosphors for Infrared Mini Lightâ€Emitting Diodes. Angewandte Chemie, 2019, 131, 2091-2094.	2.0	11
411	In Operando Transmission X-ray Microscopy Illuminated by Synchrotron Radiation for Li-Ion Batteries. ACS Energy Letters, 2018, 3, 1911-1928.	17.4	11
412	Inserting Co and P into MoS ₂ photocathodes: enhancing hydrogen evolution reaction catalytic performance by activating edges and basal planes with sulfur vacancies. Catalysis Science and Technology, 2020, 10, 6902-6909.	4.1	11
413	Epitaxial growth of high-Tc superconducting Tl-Ca-Ba-Cu-O films by liquid phase epataxial process. Physica C: Superconductivity and Its Applications, 1988, 156, 785-787.	1.2	10
414	A new series of (Tl 1â^'y Bi y)(Ca 1â^'x Y x)Sr 2 Cu 2 O z superconductors with "1122―structure. Physica C: Superconductivity and Its Applications, 1989, 162-164, 39-40.	1.2	10

#	Article	IF	CITATIONS
415	Coprecipitation process for the preparation of superconductive Biî—,Srî—,Caî—,Cu oxides. Materials Letters, 1990, 9, 105-108.	2.6	10
416	Internal Chemical Pressure Effect and Magnetic Properties of La0.6(Sr0.4â^'xBax)MnO3. Journal of Solid State Chemistry, 2001, 156, 117-121.	2.9	10
417	Studies of microstructure and ruthenium valence in the ruthenocuprates Pb2RuSr2Cu2O8Cl and (Ru,) Tj ETQq1 1	0.784314 2.9	· rgBT /Over 10
418	Effect of Lil Amount to Enhance the Electrochemical Performance of Carbon-Coated LiFePO[sub 4]. Electrochemical and Solid-State Letters, 2009, 12, A111.	2.2	10
419	Diodeâ€Like <i>I</i> – <i>V</i> Characteristics of a Nonplanar Polyaromatic Compound: a Spectroscopic Study of Isolated and Stacked Dibenzo[<i>g,p</i>]chrysene. Chemistry - an Asian Journal, 2011, 6, 1181-1187.	3.3	10
420	Synergistic Improvement in Charge Overpotential of Li–O ₂ Batteries by Oxidized Carbon Nanotubes and Cobalt Nitride Composites. Journal of Physical Chemistry C, 2018, 122, 13416-13423.	3.1	10
421	Development of upconversion nanoparticle-conjugated indium phosphide quantum dot for matrix metalloproteinase-2 cancer transformation sensing. Nanomedicine, 2019, 14, 1791-1804.	3.3	10
422	Boosting Solar Hydrogen Production of Molybdenum Tungsten Sulfide-Modified Si Micropyramids by Introducing Phosphate. ACS Applied Materials & Interfaces, 2020, 12, 41515-41526.	8.0	10
423	Capturing carbon dioxide in Na– <scp>CO₂</scp> batteries: A route for green energy. Journal of the Chinese Chemical Society, 2021, 68, 421-428.	1.4	10
424	Simultaneous construction of impermeable dual-shell stabilizing fluoride phosphors for white light-emitting diodes. Chemical Engineering Journal, 2022, 435, 134951.	12.7	10
425	Molybdenum Disulfide/Tin Disulfide Ultrathin Nanosheets as Cathodes for Sodium–Carbon Dioxide Batteries. ACS Applied Materials & Interfaces, 2022, 14, 5834-5842.	8.0	10
426	A sol-gel route to prepare Tl Ca Ba Cu O superconductor with Tc above 120 K. Physica C: Superconductivity and Its Applications, 1989, 162-164, 113-114.	1.2	9
427	The chemical control of colossal magnetoresistance (CMR) in the new two-dimensional La1.2(Sr1.8â^'xCax)Mn2O7 system. Solid State Sciences, 1999, 1, 61-65.	0.7	9
428	Short-range magnetic correlations in spinel LiMn2O4. Materials Science and Engineering B: Solid-State Materials for Advanced Technology, 2002, 95, 162-170.	3.5	9
429	An investigation of smooth nano-sized copper seed layers on TiN and TaSiN by new non-toxic electroless plating. Solid State Communications, 2003, 125, 445-448.	1.9	9
430	Systematic CuL2,3-edge and OK-edge XANES spectroscopy study on the infinite-layer superconductor system, (Sr,La)CuO2. Solid State Communications, 2008, 147, 370-373.	1.9	9
431	Crystal structure and electronic and thermal properties of TbFeAsO0.85. Applied Physics Letters, 2009, 94, 192507.	3.3	9
432	Cd-ZnGeON solid solution: the effect of local electronic environment on the photocatalytic water cleavage ability. Journal of Materials Chemistry A, 2013, 1, 7422.	10.3	9

#	Article	IF	CITATIONS
433	Enhancement of UV absorption and near-infrared emission of Er3+ in Li2SrSiO4:Ce3+, Er3+ for Ge solar spectral convertor. Optical Materials, 2014, 36, 1871-1873.	3.6	9
434	Control of Luminescence by Tuning of Crystal Symmetry and Local Structure in Mn ⁴⁺ â€Activated Narrow Band Fluoride Phosphors. Angewandte Chemie, 2018, 130, 1815-1819.	2.0	9
435	<i>In Situ</i> / <i>Operando</i> Methods of Characterizing All-Solid-State Li-Ion Batteries: Understanding Li-Ion Transport during Cycle. Journal of Physical Chemistry C, 2021, 125, 16921-16937.	3.1	9
436	Systematic treatment and evaluation of nitride phosphor with hybrid layer modification against moisture degradation. Chemical Engineering Journal, 2022, 430, 132789.	12.7	9
437	Gap surface plasmon-enhanced photoluminescence from upconversion nanoparticle-sensitized perovskite quantum dots in a metal–insulator–metal configuration under NIR excitation. Journal of Materials Chemistry C, 2022, 10, 532-541.	5.5	9
438	Spectrophotometric and polarographic methods for the determination of silicon at ng/g levels in gallium arsenide. Fresenius Zeitschrift Für Analytische Chemie, 1986, 325, 272-277.	0.8	8
439	Reversible Phase Transition of the Bi-Ca-Sr-Cu-O System between Semiconductivity and Superconductivity. Japanese Journal of Applied Physics, 1989, 28, L395-L398.	1.5	8
440	Enhancement of critical Pr ion concentration (xcr) in (La1â^'xPrx)Ba2Cu3Oz. Journal of Applied Physics, 1999, 86, 6985-6992.	2.5	8
441	Strain effect on the thermoelectric power of YBa2â [~] 'xSrxCu3O7. Physica C: Superconductivity and Its Applications, 2000, 336, 249-253.	1.2	8
442	Chemical pressure controlled colossal magnetoresistance effects in La0.6(Sr0.4â^'xCax)MnO3. Solid State Sciences, 2001, 3, 1063-1072.	0.7	8
443	Chemical pressure control of Curie temperature in La0.6(Ba0.4â^'xCax)MnO3. Materials Chemistry and Physics, 2002, 75, 26-31.	4.0	8
444	Formation mechanism and Coulomb blockade effect in self-assembled gold quantum dots. Journal of Vacuum Science & Technology an Official Journal of the American Vacuum Society B, Microelectronics Processing and Phenomena, 2004, 22, 60.	1.6	8
445	Quantitative XANES Spectroscopy Study on the Prototype Hole- and Electron-Doped High- <i>T</i> _c Superconductor Systems, (La,Sr) ₂ CuO ₄ and (Nd,Ce) ₂ CuO ₄ . Chemistry of Materials, 2008, 20, 5414-5420.	6.7	8
446	Modulating cell-uptake behavior of Au-based nanomaterials via quantitative biomolecule modification. Journal of Materials Chemistry, 2011, 21, 14821.	6.7	8
447	Enhancing the Color Rendering Index for Phosphorâ€converted White LEDs Using Cadmiumâ€Free CuInS2/ZnS QDs. Journal of the Chinese Chemical Society, 2013, 60, 801-806.	1.4	8
448	Equation of state for Eu-doped SrSi2O2N2. Journal of Chemical Physics, 2014, 141, 014705.	3.0	8
449	Vertically-aligned graphene nanowalls grown via plasma-enhanced chemical vapor deposition as a binder-free cathode in Li–O ₂ batteries. Nanotechnology, 2018, 29, 505401.	2.6	8
450	A selective drug delivery system based on phospholipid-type nanobubbles for lung cancer therapy. Nanomedicine, 2020, 15, 2689-2705.	3.3	8

#	Article	IF	CITATIONS
451	Formation and Near-Infrared Emission of CsPbI ₃ Nanoparticles Embedded in Cs ₄ PbI ₆ Crystals. ACS Applied Materials & Interfaces, 2021, 13, 34742-34751.	8.0	8
452	Linking Macro- and Micro-structural Analysis with Luminescence Control in Oxynitride Phosphors for Light-Emitting Diodes. Chemistry of Materials, 2021, 33, 7897-7904.	6.7	8
453	ESR Spectra and Low-Field Microwave Absorption in Bismuth and Thallium Based Cuprate Superconductors. Japanese Journal of Applied Physics, 1990, 29, L258-L261.	1.5	7
454	Magnetic order and spin reorientation in Nd0.45Ca0.55MnO3. Journal of Applied Physics, 1999, 85, 5588-5590.	2.5	7
455	Electrochemical studies on mixtures of LiNi0.8Co0.17Al0.03O2 and LiCoO2 cathode materials for lithium ion batteries. Solid State Communications, 2005, 133, 687-690.	1.9	7
456	Orbital ordering and valence states in(La1+xCa1â^'x)CoRuO6double perovskites. Physical Review B, 2005, 72, .	3.2	7
457	Chemical control of high-Tcsuperconductivity of the triple-fluorite-layer copper oxide(Cu,Mo)Sr2(Ce,R)3Cu2O11+Î′(R=Y,La–Yb). Physical Review B, 2005, 72, .	3.2	7
458	Pressure dependence of the Sr2Si5N8:Eu2+ luminescence. Journal of Luminescence, 2015, 159, 183-187.	3.1	7
459	Near-Infrared-Activated Fluorescence Resonance Energy Transfer-Based Nanocomposite to Sense MMP2-Overexpressing Oral Cancer Cells. ACS Omega, 2018, 3, 1627-1634.	3.5	7
460	Optimizing the Lithium Phosphorus Oxynitride Protective Layer Thickness on Lowâ€Grade Composite Siâ€Based Anodes for Lithiumâ€Ion Batteries. ChemistrySelect, 2018, 3, 729-735.	1.5	7
461	Thermal stabilization and energy transfer in narrow-band red-emitting Sr[(Mg ₂ Al ₂) _{1â^{~^}y} (Li ₂ Si ₂) _y N <sub Journal of Materials Chemistry C, 2018, 6, 5975-5983.</sub 	>4 s/s ub>]]:Eux sup>2+
462	Thermal quenching of Ce3+luminescence in the cuspidine-type oxide nitride compounds Y4Si2â^'xAlxO7+xN2â~'x. Journal of Luminescence, 2018, 193, 125-132.	3.1	7
463	Graphene oxide @ nickel phosphate nanocomposites for photocatalytic hydrogen production. Chemical Engineering Journal Advances, 2021, 6, 100105.	5.2	7
464	Microstructure, thermoelectric power and magnetic irreversibility of coprecipitated YBa2Cu4O8 powders. Solid State Communications, 1992, 81, 767-770.	1.9	6
465	Chemical size effect on the magnetic and electrical properties of colossal magnetoresistance La1.2(Sr1.8â€â^â€xCax)Mn2O7 materials. Journal of the Chemical Society Dalton Transactions, 1999, , 623-	628 <mark>.</mark>	6
466	Studies into the phase transformation of Bi-2223 precursor powders using X-ray diffraction and SQUID susceptibility measurements. IEEE Transactions on Applied Superconductivity, 2001, 11, 3182-3185.	1.7	6
467	Effect of Pb doping in high-Tc Bi2Sr2CaCu2Oy superconductors studied by X-ray absorption near-edge structure spectroscopy. Physica C: Superconductivity and Its Applications, 2001, 364-365, 567-570.	1.2	6
468	Synthesis and magnetic properties of multilayer Ni/Cu and NiFe/Cu nanowires. Pramana - Journal of Physics, 2006, 67, 85-91.	1.8	6

#	Article	IF	CITATIONS
469	High pressure photoluminescence of Ce3+-doped (Y1.725Tb0.575Ce0.05Gd0.65)Al5O12. Optical Materials, 2008, 30, 722-724.	3.6	6
470	Formation, crystal growth and colour appearance of Mimetic Tianmu glaze. Ceramics International, 2016, 42, 7506-7513.	4.8	6
471	Structural Evolution and Effect of the Neighboring Cation on the Photoluminescence of Sr(LiAl 3) 1â^' x (SiMg 3) x N 4 :Eu 2+ Phosphors. Angewandte Chemie, 2019, 131, 7849-7854.	2.0	6
472	Pressure-controlled chemical vapor deposition of graphene as catalyst for solar hydrogen evolution reaction. Catalysis Today, 2019, 335, 395-401.	4.4	6
473	Progress and Viewpoints of Multifunctional Composite Nanomaterials for Glioblastoma Theranostics. Pharmaceutics, 2022, 14, 456.	4.5	6
474	Transport, magnetic and microstructural characteristics in the high-critical-temperature superconductor Bi-Ca-Sr-Cu-O. Physica C: Superconductivity and Its Applications, 1988, 152, 345-348.	1.2	5
475	Growth of Bi-Ca-Sr-Cu-O epitaxial layer by liquid phase epitaxial process. Physica C: Superconductivity and Its Applications, 1988, 156, 197-199.	1.2	5
476	Synthesis of High-TcYBa2Cu3O7-xSuperconductors at a Low Annealing Temperature from a Glass Precursor. Japanese Journal of Applied Physics, 1989, 28, L41-L44.	1.5	5
477	Determination of the concentrations of trace and doping elements in GaAs by neutron activation analysis. Journal of Radioanalytical and Nuclear Chemistry, 1990, 141, 317-326.	1.5	5
478	Further measurements on the Tl0.5Pb0.5Sr2(Ca1â^'yYy)Cu2O7â^'δ system Pb NMR and magnetic susceptibility. Physica C: Superconductivity and Its Applications, 1995, 244, 207-213.	1.2	5
479	The study of the hole distribution in high- 1212-type cuprates via x-ray absorption spectroscopy. Superconductor Science and Technology, 1998, 11, 1028-1031.	3.5	5
480	XANES STUDY OF THE VALENCE OF Pb IN (Tl0.5Pb0.5)Sr2Ca1-xYxCu2O7-δ. International Journal of Modern Physics B, 1999, 13, 3693-3696.	2.0	5
481	Title is missing!. Journal of Low Temperature Physics, 2003, 131, 1205-1210.	1.4	5
482	Soft-x-ray absorption spectroscopy of heterostructured high-Tcsuperconducting nanohybrids:Xâ^'Bi2Sr2CaCu2O8[X=I,HgI2, and(Pyâ^'CH3)2HgI4]. Physical Review B, 2005, 71, .	3.2	5
483	Morphology and Surface Plasma Changes of Au–Pt Bimetallic Nanoparticles. Journal of Nanoscience and Nanotechnology, 2006, 6, 1411-1415.	0.9	5
484	Hole doping into Co-12s2 copper oxides with s fluorite-structured layers between CuO2 planes. Journal of Solid State Chemistry, 2006, 179, 632-645.	2.9	5
485	Structural, electronic and magnetic properties of ErFeMn and ErFeMnH4.7compounds. New Journal of Physics, 2007, 9, 271-271.	2.9	5
486	ZrNi5-based hydrogenated phases formed under high hydrogen pressure conditions. Applied Surface Science, 2011, 257, 8237-8240.	6.1	5

Ru-Sнi Liu

#	Article	IF	CITATIONS
487	The substitution of the platinum counter electrode in a plasmonic photoelectrochemical system with near-infrared absorption for solar water splitting. RSC Advances, 2016, 6, 103160-103168.	3.6	5
488	Stable Luminous Organic–Inorganic Hybrid Manganese Halide Nanostructures for Light-Emitting Diodes. ACS Applied Nano Materials, 2022, 5, 4623-4628.	5.0	5
489	Resistive, magnetic, and structural studies of Tl0.5Pb0.5(Ca1â^'xMx)Sr2Cu2Oycompounds withMequal to the natural mixture of rareâ€earth elements. Applied Physics Letters, 1989, 55, 2029-2031.	3.3	4
490	Synthesis of a 90 K Y2Ba4Cu7O15â^'x superconductor under ambient pressure by triethylammoniumoxalate co-precipitation. Physica C: Superconductivity and Its Applications, 1993, 215, 435-438.	1.2	4
491	Soft X-ray absorption study of (Nd1.05â^'xPrx)Ba1.95Cu3O7 using synchrotron radiation. Chemical Physics Letters, 1998, 294, 209-216.	2.6	4
492	Crystal structure and magnetic properties of the double perovskite (Sr2â^'xCax)FeMoO6 (0⩽x⩽1.0). Jourr of Magnetism and Magnetic Materials, 2002, 239, 164-166.	າal 2.3	4
493	XANES and wet-chemical analyses of the charge balance in (Hg,Pb)(Ba,Sr)2Ca2Cu3O8+z. Physica C: Superconductivity and Its Applications, 2003, 392-396, 93-98.	1.2	4
494	Effect of Sr-for-Ba isovalent substitution on the local structure, hole distribution and magnetic irreversibility of Cu(Ba,Sr)2YbCu2O6.95(2). Journal of Solid State Chemistry, 2004, 177, 1925-1932.	2.9	4
495	Enhancement of ferromagnetic interactions in multiferric (Tb/sub 1-x/Na/sub x/)MnO/sub 3/ system. IEEE Transactions on Magnetics, 2005, 41, 2751-2753.	2.1	4
496	Oxygen nonstoichiometry and valence of copper in the Cu-1222 superconductor. Journal of Solid State Chemistry, 2005, 178, 1705-1711.	2.9	4
497	SYNTHESIS, STRUCTURAL AND MAGNETIC PROPERTIES OF DOUBLE PEROVSKITES Sr2CrWO6. International Journal of Modern Physics B, 2005, 19, 537-540.	2.0	4
498	Transformation of Co nanodisks to Co caterpillars. Journal of Magnetism and Magnetic Materials, 2006, 304, e19-e21.	2.3	4
499	Influence of Oxygen Defects on the Crystal Structure and Magnetic Properties of the (Tb1-xNax)MnO3-y(0 ≤≤0.3) System. Inorganic Chemistry, 2007, 46, 4575-4582.	4.0	4
500	Magnetic ordering of Mn and Ru in (La0.52Ba0.48) (Mn0.51Ru0.49)O3. Physica Status Solidi (B): Basic Research, 2007, 244, 2233-2241.	1.5	4
501	Comparative XANES study on the two electron-doped high-Tc superconductor systems, (Sr,La)CuO2 and (Nd,Ce)2CuO4. Journal of Solid State Chemistry, 2009, 182, 1217-1221.	2.9	4
502	Formation of Hydrides in (Ti _{1â^'<i>x</i>} Zr _{<i>x</i>})Co _{2.00} (0 <) Tj ETQq	0 0 0 rgB⊺ 4.0	T /Overlock :
503	Preparation and Characterization of Ni or Co/Cu Multilayer Nanowires. Journal of the Chinese Chemical Society, 2010, 57, 888-891.	1.4	4

⁵⁰⁴Functional electroless gold Ohmic contacts in light emitting diodes. Applied Physics Letters, 2011, 99,
063511.3.34

#	Article	IF	CITATIONS
505	Highly efficient urchin-like bimetallic nanoparticles for photothermal cancer therapy. SPIE Newsroom, 0, , .	0.1	4
506	NIR-assisted orchid virus therapy using urchin bimetallic nanomaterials in phalaenopsis. Advances in Natural Sciences: Nanoscience and Nanotechnology, 2013, 4, 045006.	1.5	4
507	Formation of Sr ₂ Si ₅ N ₈ :Eu ²⁺ and Its Transformation to SrSi ₆ N ₈ :Eu ²⁺ ControlledÂby Temperature and Gas Pressure. Journal of the American Ceramic Society, 2015, 98, 2662-2669.	3.8	4
508	Phosphors for White LEDs. , 2017, , 181-222.		4
509	In-Situ Transmission X-Ray Microscopy Probed by Synchrotron Radiation for Li-Ion Batteries. Frontiers in Energy Research, 2018, 6, .	2.3	4
510	Characterization of Bi Pb Sb Ca Sr Cu O superconductor sintered in controlled atmosphere. Physica C: Superconductivity and Its Applications, 1989, 162-164, 911-912.	1.2	3
511	Local-magnetic-moment variation in pure and impure phases of Tl-Ca-Ba-Cu-O superconductors. Journal of Physics and Chemistry of Solids, 1990, 51, 65-71.	4.0	3
512	Synthesis, at ambient pressure, of the 80 K superconductor YBa2Cu4O8 by triethylammonium oxalate co-precipitation. Journal of the Chemical Society Chemical Communications, 1991, , 664.	2.0	3
513	A study of the orientation dependence of the 63Cu nuclear magnetic resonance in the (Tl0.5Pb0.5)Sr2(Ca1â^'yYy)Cu2O7-Î system. Physica C: Superconductivity and Its Applications, 1994, 220, 93-100.	1.2	3
514	Charge distribution in (Tl,Pb)Sr2Ca2Cu3O9â^ʾσ (Tc=124K): an 17O NMR study. Physica C: Superconductivity and Its Applications, 1994, 235-240, 1709-1710.	1.2	3
515	Electron-spin-resonance studies of the hole-doping effect on (Tl0.5Pb0.5)Sr2(Ca1â^'xYx)Cu2O7high-Tcsuperconductors. Physical Review B, 1995, 52, 12883-12889.	3.2	3
516	Enhancement of Zero Resistance Temperature above 90 K and Hole Distribution in (Hg0.5Pb0.5)Sr2(Ca0.7Y0.3)Cu2O7-1´ via Chemical Substitution of Ba into Sr Sites. Inorganic Chemistry, 1997, 36, 1378-1382.	4.0	3
517	Chemical Control of Underdoped and Overdoped States in Y(Ba2 â~' y Sr y)Cu3O6 + δ. Journal of Superconductivity and Novel Magnetism, 1998, 11, 563-567.	0.5	3
518	Tilted antiferromagnetic ordering of Mn in Nd0.62Ca0.38MnO3. Journal of Applied Physics, 1998, 83, 7345-7347.	2.5	3
519	New advanced magnetic La1.2(Sr1.8â^'xCax)Mn2O7 compounds with colossal magnetoresistance. Journal of Magnetism and Magnetic Materials, 2000, 209, 113-115.	2.3	3
520	Controlling Length and Monitoring Growth of Gold Nanorods. Journal of the Chinese Chemical Society, 2006, 53, 1343-1348.	1.4	3
521	High-resolution XANES study of Eu(Ba1â^'xRx)2Cu3O7+δ (R = Eu, Pr). New Journal of Physics, 2006, 8, 215-215.	2.9	3
522	Large positive magnetoresistance effect below Curie temperature in In1.90â^'xMn0.1SnxO3. Journal of Applied Physics, 2007, 101, 09H121.	2.5	3

#	Article	IF	CITATIONS
523	Effects of oxygen deficiency on the magnetic ordering of Mn in Tb0.9Na0.1MnO2.9. Journal of Physics Condensed Matter, 2008, 20, 104234.	1.8	3
524	Neutron polarization analysis on the multiferroic TbMn2O5. Physica B: Condensed Matter, 2009, 404, 2517-2519.	2.7	3
525	Structural, electronic and magnetic properties of YFeMnH5. International Journal of Hydrogen Energy, 2011, 36, 1046-1052.	7.1	3
526	Facile dental resin composites with tunable fluorescence by tailoring Cd-free quantum dots. RSC Advances, 2013, 3, 16639.	3.6	3
527	Syntheses and properties of several metastable and stable hydrides derived from intermetallic compounds under high hydrogen pressure. Applied Surface Science, 2016, 388, 723-730.	6.1	3
528	Synergetic effect-triggered performance promotion of Sr3â^'xBaxP5N10Cl:Eu2+ phosphors. Journal of Materials Chemistry C, 2021, 9, 12063-12067.	5.5	3
529	Na@C composite anode for a stable Na NZSP interface in solid-state Na–CO2 battery. Journal of Alloys and Compounds, 2022, 922, 166123.	5.5	3
530	Formation of YBa 2 BiO 6 and its effect on the superconductivity in Bi replaced YBa 2 Cu 3 O y. Physica C: Superconductivity and Its Applications, 1989, 162-164, 71-72.	1.2	2
531	Tc enhancement of the (Tl, Pb, Bi)Sr-Ca-Cu-O and Tl-Ba-Ca-Cu-O systems. Applied Superconductivity, 1993, 1, 527-534.	0.5	2
532	The growth of large-area superconducting YBa2Cu3O7â^'x thin films by pulsed laser ablation. Materials Chemistry and Physics, 1996, 43, 66-69.	4.0	2
533	Electronic structure in (Hg0.5Pb0.5)Sr2(Ca1â [~] 'xYx)Cu2O7 compounds studied by soft X-ray absorption spectroscopy. Physica C: Superconductivity and Its Applications, 1996, 272, 180-186.	1.2	2
534	Interaction between a cylindrical superconducting impurity and a vortex in a type-II superconductor. Physica C: Superconductivity and Its Applications, 1997, 275, 135-140.	1.2	2
535	Charge transfer process in Tl2Ba2Ca2Cu3O10 and Tl2Ba2CaCu2O8 thin films probed by polarized X-ray absorption spectroscopy. Chemical Physics Letters, 1997, 276, 303-308.	2.6	2
536	Title is missing!. Journal of Superconductivity and Novel Magnetism, 1998, 11, 53-57.	0.5	2
537	Structure and Magnetoresistance of Pr0.7(Sr0.3-yCay) MnO3. International Journal of Modern Physics B, 1998, 12, 1763-1771.	2.0	2
538	Substitution effects in Bi2Sr2(Ca1â^'xYx)Cu2O8+δ studied by X-ray absorption spectroscopy. Physica C: Superconductivity and Its Applications, 2000, 341-348, 383-386.	1.2	2
539	Superlattice structures between YBa2Cu3O7â^î´ and (Pb,Cu)Sr2(Ca,Y)Cu2O7â^î´ high-Tc cuprates. Solid State Sciences, 2000, 2, 645-649.	0.7	2
540	Chemical control of colossal magnetoresistance in manganites. Materials Chemistry and Physics, 2001, 72, 281-285.	4.0	2

#	Article	IF	CITATIONS
541	Coulomb Blockade Effect in a Nano-Sized Gold Chain. International Journal of Modern Physics B, 2003, 17, 3637-3639.	2.0	2
542	Electrochemical and in situ XANES studies of a LiNi0.8Co0.17Al0.03O2 cathode material. Solid State Communications, 2004, 132, 273-277.	1.9	2
543	Neutron diffraction study of multiferroic Tb0.85Na0.15MnO3â^'y. Journal of Magnetism and Magnetic Materials, 2007, 310, 1151-1153.	2.3	2
544	Synthesis and characterization of long gold nanorods. IEEJ Transactions on Electrical and Electronic Engineering, 2007, 2, 468-472.	1.4	2
545	A Simplified Synthetic Experiment of YBa2Cu3O7–x Superconductor for First-Year Chemistry Laboratory. Journal of Chemical Education, 2008, 85, 825.	2.3	2
546	Calorimetric properties of C14 and C15 YMn2 and YMn2(H,D)6. International Journal of Hydrogen Energy, 2011, 36, 2285-2290.	7.1	2
547	Hydrides Formed in ZrCo2 – Based Intermetallic Compounds Under High Hydrogen Pressure / Wodorki Wytwarzane Pod Wysokimi Cisnieniami Wodoru Ze Zwiazków Miedzymetalicznych Na Osnowie ZrCo2. Archives of Metallurgy and Materials, 2013, 58, 223-226.	0.6	2
548	Nanosized-Fe 3 PtN supported on nitrogen-doped carbon as electro-catalyst for oxygen reduction reaction. International Journal of Hydrogen Energy, 2017, 42, 15761-15769.	7.1	2
549	Editorial: Electrode Materials for Lithium and Post-Lithium Rechargeable Batteries. Frontiers in Materials, 2020, 7, .	2.4	2
550	Dimensional and Chemical Control of Colossal Magnetoresistance in New Manganites. Japanese Journal of Applied Physics, 2000, 39, 473.	1.5	2
551	Halideâ€type Liâ€ion conductors: Future options for highâ€voltage allâ€solidâ€state batteries. Journal of the Chinese Chemical Society, 2022, 69, 1233-1241.	1.4	2
552	Growth of high Tc-superconducting Y-Ba-Cu-O thin films by a chemical spray pyrolysis method. Physica C: Superconductivity and Its Applications, 1988, 153-155, 804-805.	1.2	1
553	Superconductivity Above 100 K in Tl-Pb-Ca-R-Sr-Cu-O System. Molecular Crystals and Liquid Crystals Incorporating Nonlinear Optics, 1990, 184, 17-24.	0.3	1
554	The chemical control of high-Tc superconductivity: Metal-superconductor-insulator transition in (Tl1â^'yPby)Sr2(Ca1â^'xYx)Cu2O7. Journal of Electronic Materials, 1993, 22, 1199-1203.	2.2	1
555	Crystal structure and superconductivity in the Hg-containing Ba- and Sr-based cuprates. Physica C: Superconductivity and Its Applications, 1994, 235-240, 897-898.	1.2	1
556	Comparison of irreversibility lines of silver-sheathed Bi-2223, Tl-1223 and Tl-1234 superconducting tapes. Materials Chemistry and Physics, 1996, 43, 83-85.	4.0	1
557	Hole states in (Cd0.5Pb0.5)Sr2(CaxY1â€â^'â€x)Cu2O7 studied by X-ray absorption spectroscopy. Journal of th Chemical Society Dalton Transactions, 1998, , 2569-2572.	1.1	1
558	Cu K-Edge Study of (Tl0.5Pb0.5)Sr2Ca1-xYxCu2O7-δ. International Journal of Modern Physics B, 1998, 12, 3296-3298.	2.0	1

#	Article	IF	CITATIONS
559	Hole states in Eu0.9 â^` xPrxCa0.1BaSrCu3O7 â^` δ studied by X-ray absorption spectroscopy. Journal Chemical Society Dalton Transactions, 1999, , 2065-2070.	of the	1
560	Title is missing!. Journal of Low Temperature Physics, 2003, 131, 381-386.	1.4	1
561	Optical studies of lattice and charge excitations in La1.2(Sr1.8â^'xCax)Mn2O7. Journal of Applied Physics, 2003, 93, 6894-6896.	2.5	1
562	Synthesis and Characterization of Double Perovskites Sr2FeMO6 (M = Mo, W). International Journal of Modern Physics B, 2003, 17, 3500-3502.	2.0	1
563	Synthesis and Characterization of Novel Au(core)-Au/Pt Alloy(shell) Nanostructure. Materials Research Society Symposia Proceedings, 2004, 818, 299.	0.1	1
564	Co valence by K-edge X-ray absorption spectroscopy, magnetic properties, and structure of polycrystalline bulk Zn/sub 1-x/Co/sub x/O. IEEE Transactions on Magnetics, 2005, 41, 2727-2729.	2.1	1
565	Chemical Control of Hole Distribution and Superconductivity in $(Cu,Mo)Sr2(Ce,R)sCu2O5+2s+\hat{I}$ (s = 2,) Tj ETQq1	1.0,7843 6.7	14 rgBT /O∨
566	Local structural characterization of gold nanowires using extended X-ray absorption fine structure spectroscopy. Chemical Physics Letters, 2006, 428, 93-97.	2.6	1
567	Frontispiece: Mesoporous Silica Particles Integrated with Allâ€Inorganic CsPbBr ₃ Perovskite Quantumâ€Dot Nanocomposites (MPâ€PQDs) with High Stability and Wide Color Gamut Used for Backlight Display. Angewandte Chemie - International Edition, 2016, 55, .	13.8	1
568	Introduction to the Basic Properties of Luminescent Materials. , 2017, , 1-29.		1
569	Cobalt Diselenide Nanorods Grafted on Graphitic Carbon Nitride: A Synergistic Catalyst for Oxygen Reactions in Rechargeable Liâ^'O2 Batteries. ChemElectroChem, 2018, 5, 5-5.	3.4	1
570	Pâ€121: Successive and Scalable Synthesis of Highly Stable Cs ₄ PbBr ₆ Perovskite Microcrystal by Microfluidic System and Their Application in Backlight Display. Digest of Technical Papers SID International Symposium, 2018, 49, 1664-1666.	0.3	1
571	Correlated N/O anion orders in melilite phosphors. Journal of Solid State Chemistry, 2020, 284, 121198.	2.9	1
572	Dual-emission Eu-doped Ca2â´'xSrxPN3 nitridophosphate phosphors prepared by hot isostatic press. Journal of Materials Chemistry C, 2021, 9, 8158-8162.	5.5	1
573	Nearâ€Infrared Nanophosphor Embedded in Mesoporous Silica Nanoparticle with High Lightâ€Harvesting Efficiency for Dual Photosystem Enhancement. Angewandte Chemie, 2021, 133, 7031-7035.	2.0	1
574	Coexistence of paramagnetism and superconductivity in (Gd 0.2 Ca 0.8)Sr 2 (Tl 0.5 Pb 0.5)Cu 2 O y. Physica C: Superconductivity and Its Applications, 1989, 162-164, 323-324.	1.2	0
575	Rapid calcination and post-annealing of the Biî—,Srî—,Caî—,Cuî—,O High-Tc superconductor. Materials Letters, 1989, 8, 293-296.	2.6	0
576	Superconductivity in Pb-based 1212 cuprates; evidence for under-doping from thermoelectric power. Solid State Communications, 1993, 87, 31-34.	1.9	0

#	Article	IF	CITATIONS
577	Interfacial Study ofTl2Ba2Ca2Cu3O10Thin Films on Silver Foil. Japanese Journal of Applied Physics, 1994, 33, 3900-3901.	1.5	0
578	Flux dynamics and critical currents of high Tc tapes. Physica C: Superconductivity and Its Applications, 1994, 235-240, 3417-3418.	1.2	0
579	Erratum to "Comparison of irreversibility lines of silver-sheathed Bi-2223, Tl-1223 and Tl-1234 superconducting tapes―[Materials Chemistry and Physics 43 (1996) 83-85]. Materials Chemistry and Physics, 1996, 46, 103.	4.0	0
580	The study of electronic structure in new Hg-based Sr-containing 1212-typed (Hg0.5Pb0.5)Sr2(Ca1â^'xYx)Cu2O7 superconductors. Physica C: Superconductivity and Its Applications, 1997, 282-287, 961-962.	1.2	0
581	Hole states in oxycarbonate high-Tc superconductor (Tl0.8Cr0.2)Sr4Cu2(CO3)O7 probed by soft X-ray absorption spectroscopy. Physica C: Superconductivity and Its Applications, 1997, 277, 145-151.	1.2	0
582	Hole distribution in the underdoped, optimally doped, and overdoped superconductors (Tl0.5Pb0.5)Sr2(Ca1â^'xYx)Cu2O7. Physica C: Superconductivity and Its Applications, 1997, 282-287, 981-982.	1.2	0
583	Superlattice structures in solid solution of high-Tc YBa2Cu3O7â~'δ and (Pb,Cu)Sr2(Ca,Y)Cu2O7â~'δ superconductors. Journal of Physics and Chemistry of Solids, 2001, 62, 1847-1859.	4.0	0
584	`Maturization' of high-Tc precursor powders for use in superconducting tapes. Physica C: Superconductivity and Its Applications, 2002, 372-376, 1167-1170.	1.2	0
585	Title is missing!. Journal of Low Temperature Physics, 2003, 131, 613-618.	1.4	0
586	Internal oxidation in Bi2.1 – xPbxSr2 – yCa1 – zYy + zCu2O8 + d solid solutions. Mendeleev Communications, 2004, 14, 181-182.	1.6	0
587	Synthesis and Luminescent Properties of a New Yellowish-Orange Afterglow Phosphor Y2O2S:Ti,Mg ChemInform, 2004, 35, no.	0.0	0
588	Short range magnetic corrections in spinel Li(Mn0.976Co0.024)2O4. Journal of Magnetism and Magnetic Materials, 2004, 272-276, 833-834.	2.3	0
589	Magnetic order and spin fluctuations in Ni-rich Li0.9Ni1.1O2. Physica B: Condensed Matter, 2006, 385-386, 432-434.	2.7	0
590	Hole states of X-Bi2Sr2CaCu2O8 [X=I, HgI2, and (Py-CH3)2HgI4] probed by O K-edge X-ray absorption spectroscopy. Journal of Physics and Chemistry of Solids, 2006, 67, 223-226.	4.0	0
591	Formation of nanostructured cobalt wires with Chinese caterpillar type structure. Journal of Vacuum Science & Technology B, 2006, 24, 1440.	1.3	0
592	Control of hole distribution through isovalent R-cation substitution in Cu2Ba2RCu2O8 superconductors. Applied Physics Letters, 2007, 90, 032511.	3.3	0
593	A Special Issue for the Electrical Energy Storage and Conversion…. Journal of the Chinese Chemical Society, 2012, 59, 1159-1162.	1.4	0
594	Xâ€ray Absorption Spectroscopy Approaches to Electronic State and Coordination Type of Lithium Phosphorus Oxynitride Thin Films. Journal of the Chinese Chemical Society, 2012, 59, 1270-1274.	1.4	0

Ru-Sнi Liu

#	Article	IF	CITATIONS
595	Introduction to Energy Storage Subâ€program of National Science and Technology Programâ€Energy in Taiwan. Journal of the Chinese Chemical Society, 2012, 59, 1173-1180.	1.4	0
596	Hydrogen Generation: Plasmonic ZnO/Ag Embedded Structures as Collecting Layers for Photogenerating Electrons in Solar Hydrogen Generation Photoelectrodes (Small 17/2013). Small, 2013, 9, 2830-2830.	10.0	0
597	Plasmonic zinc oxide/silver photoelectrode for green hydrogen production. SPIE Newsroom, 2013, , .	0.1	0
598	Photodynamic Therapy: Minimizing the Heat Effect of Photodynamic Therapy Based on Inorganic Nanocomposites Mediated by 808 nm Nearâ€Infrared Light (Small 21/2017). Small, 2017, 13, .	10.0	0
599	Characteristics and Properties of A(I,II)M(IV)F6 Fluoride Phosphors. , 2017, , 371-398.		0
600	Plasmonic Nanoparticles: Plasmon-Enhanced Electrocatalytic Properties of Rationally Designed Hybrid Nanostructures at a Catalytic Interface (Adv. Mater. Interfaces 2/2019). Advanced Materials Interfaces, 2019, 6, 1970011.	3.7	0
601	Study on the surface modification of spinel LiNi0.45Cr0.1Mn1.45O4. Journal of Alloys and Compounds, 2020, 821, 153418.	5.5	0
602	Plasmonic Photocatalyst for Photodegradation with Spinning Optical Disk Reactor. , 2014, , .		0
603	Phosphors for White LEDs. , 2016, , 1-42.		0
604	(Invited) Photoelectrochemical Hydrogen Evolution Using Heterostructure of Si with Binary Cobalt Sulï¬De or Ternary Cobalt Phosphosulï¬De. ECS Meeting Abstracts, 2017, , .	0.0	0
605	(Invited) Narrow Band Emission of Nitrides Phosphors and All Inorganic Perovskite Quantum Dots for the Application in Light Emitting Diodes. ECS Meeting Abstracts, 2017, , .	0.0	0